

# Neuron

## Leaky Gate Model: Intensity-Dependent Coding of Pain and Itch in the Spinal Cord

### Highlights

- *Grp*<sup>+</sup> neurons receive monosynaptic input from both pain and itch primary neurons
- Intensity-dependent coding of pain by *Grp*<sup>+</sup> neurons
- *Grp*<sup>+</sup> neurons form “leaky gate” to negatively regulate pain transmission
- Loss of *Grp*<sup>+</sup> neurons decreases itch and increases pain

### Authors

Shuohao Sun, Qian Xu,  
Changxiong Guo, Yun Guan, Qin Liu,  
Xinzhong Dong

### Correspondence

xdong2@jhmi.edu

### In Brief

A small subset of spinal interneurons labeled by *Grp* intensity-dependently codes for pain and itch. Accordingly, Sun et al. propose a new model in which *Grp*<sup>+</sup> neurons code for itch but inhibit strong pain through a “leaky gate.”



# Leaky Gate Model: Intensity-Dependent Coding of Pain and Itch in the Spinal Cord

Shuohao Sun,<sup>1,5</sup> Qian Xu,<sup>1,5</sup> Changxiong Guo,<sup>4</sup> Yun Guan,<sup>2</sup> Qin Liu,<sup>4</sup> and Xinzhong Dong<sup>1,3,6,\*</sup>

<sup>1</sup>The Solomon H. Snyder Department of Neuroscience and Center for Sensory Biology

<sup>2</sup>Department of Anesthesiology and Critical Care Medicine

<sup>3</sup>Howard Hughes Medical Institute

Johns Hopkins University School of Medicine, Baltimore, MD 21205, USA

<sup>4</sup>Department of Anesthesiology and the Center for the Study of Itch, Department of Ophthalmology and Visual Sciences, Washington University School of Medicine, St Louis, MO, 63110, USA

<sup>5</sup>Co-first author

<sup>6</sup>Lead Contact

\*Correspondence: [xdong2@jhmi.edu](mailto:xdong2@jhmi.edu)

<http://dx.doi.org/10.1016/j.neuron.2017.01.012>

## SUMMARY

Coding of itch versus pain has been heatedly debated for decades. However, the current coding theories (labeled line, intensity, and selectivity theory) cannot accommodate all experimental observations. Here we identified a subset of spinal interneurons, labeled by gastrin-releasing peptide (*Grp*), that receive direct synaptic input from both pain and itch primary sensory neurons. When activated, these *Grp*<sup>+</sup> neurons generated rarely seen, simultaneous robust pain and itch responses that were intensity dependent. Accordingly, we propose a “leaky gate” model in which *Grp*<sup>+</sup> neurons transmit both itch and weak pain signals; however, upon strong painful stimuli, the recruitment of endogenous opioids works to close this gate, reducing overwhelming pain generated by parallel pathways. Consistent with our model, loss of these *Grp*<sup>+</sup> neurons increased pain responses while itch was decreased. Our new model serves as an example of non-monotonic coding in the spinal cord and better explains observations in human psychophysical studies.

## INTRODUCTION

Pain and itch are two distinct yet related sensations. Both pain and itch are detected by small-diameter dorsal-root ganglia (DRG) neurons and transmitted to the spinal cord dorsal horn, yet they trigger distinct behavioral responses. Pain generates a withdrawal response to avoid tissue damage, while itch elicits scratching to remove irritants. Pain can suppress itch, which is demonstrated when the mechanical pain generated by scratching relieves the itchy sensation (Davidson et al., 2009). Itch, however, can rarely suppress pain. On the cellular level, neurons responsive to itchy stimuli in both DRG and the spinal cord can also be activated by pain (Akiyama et al., 2009a; Davidson

et al., 2007; Liu et al., 2009; Schmelz et al., 2003), begging the question of how these two sensations are distinguished.

Debates about pain and itch coding have been ongoing for decades. One major theory, the intensity theory, claims that polymodal sensory neurons respond to both painful and itchy stimuli. The same group of neurons can be stimulated strongly or weakly to generate pain or itch sensations, respectively (Lewis et al., 1927; Von Frey, 1922). However, weaker painful stimuli or stronger itchy stimuli fail to turn into a different sensation, thus raising questions about the intensity theory (Handwerker et al., 1991; Ochoa and Torebjörk, 1989; Tuckett, 1982). Another major theory is the labeled-line theory, which argues that different senses are coded by mutually exclusive populations (Norrzell et al., 1999; Schmelz et al., 1997). However, the fact that itch-responsive neurons are also activated by painful stimuli argues against the labeled-line theory. A modified labeled-line theory, termed the selectivity theory, incorporates the existence of polymodal sensory neurons (Handwerker, 1992; McMahon and Koltzenburg, 1992). The selectivity theory suggests that itchy stimuli specifically activate itch-selective neurons to generate itch sensation, while painful stimuli activate both itch-selective neurons and a larger nociceptive population whose activation inhibits itch to produce only pain sensation.

Recent studies largely support this modified labeled-line theory. In DRG, Han et al. (2013) confirmed the existence of “itch-selective” neurons by showing that the activation of the *MrgprA3*<sup>+</sup> primary sensory neurons generated itch but not pain responses, while its ablation impaired itch and spared pain (Han et al., 2013). Further along this same labeled line, the “itch-selective” neurons in the spinal cord are proposed to be the gastrin-releasing peptide receptor (GRPR)-positive population. The loss of the GRPR<sup>+</sup> neurons abolished most itch responses but spared pain responses (Sun et al., 2009). In addition, brain natriuretic peptide (BNP) is suggested to be the itch-specific neurotransmitter, signaling between itch-selective cells in DRG and itch-selective cells in the spinal cord (Mishra and Hoon, 2013). However, in human psychophysical studies, most chemical-induced itch sensations are accompanied by weaker nociceptive sensations (burning, pricking, stinging, etc.) (LaMotte et al., 2014; Liu et al., 2012; Sikand et al., 2009,

2011a). These mixed sensations raise questions about the “selectivity” of itch pathways.

Although we cannot deny the beauty of simplicity, the anatomical structure of the spinal cord dorsal horn seems to suggest a more complicated and integrative organization of sensory circuits than labeled lines. Unlike pseudo-unipolar DRG neurons, which all serve output functions, only a small subset of superficial dorsal-horn neurons transmit signals further to the brain (Spike et al., 2003). The remaining majority are interneurons forming interlacing local circuitries whose functions remain largely elusive. Here we attempted to reveal the functions of dorsal-horn circuits as they related to pain and itch. Second-order neurons are the first step in the spinal circuitry, receiving direct synaptic input from DRG neurons. We identified a subset of second-order neurons, positive for *Grp*, that receive direct synaptic inputs from both pain and itch primary sensory neurons. Surprisingly, the activation of the *Grp*<sup>+</sup> neurons generated both pain and itch responses, with the pain coding being intensity dependent. These data led us to this “leaky gate” model, which provides a refined theory for pain and itch coding in the spinal cord and better explains results from human psychophysics experiments.

## RESULTS

### Genetic Labeling of Itch Second-Order Neurons in the Spinal Cord

Previously, we discovered that axons of *MrgprA3*<sup>+</sup> itch primary sensory neurons selectively terminate in lamina II of spinal cord (Han et al., 2013). To identify genetic markers of second-order neurons that form synapses directly with *MrgprA3*<sup>+</sup> neurons, we utilized transgenic mouse lines with Cre recombinase expression under specific neuronal gene promoters; these lines were generated using bacterial artificial chromosome (BAC)-based transgenic technology by the Gene Expression Nervous System Atlas (GENSAT) project (Gong et al., 2003). Upon screening all GENSAT Cre lines with expression in the spinal cord dorsal horn, we focused on a promising target, *Grp*. *Grp* has previously been implicated in itch transmission. *Grp* was reported to express in DRG, but not in spinal cord, and had been proposed to provide input to GRPR<sup>+</sup> neurons (Sun and Chen, 2007). However, recent studies suggest that *Grp* instead expresses in spinal cord dorsal horn, not the DRG (Fleming et al., 2012; Solorzano et al., 2015).

Consistent with the recent studies, we found that *Grp*<sup>Cre</sup> expression was restricted to the superficial lamina of the spinal cord, and we could not detect *Grp*<sup>Cre</sup> expression in DRG (Figures 1A and 1B), when visualized with *ROSA26*<sup>L<sup>SL</sup>-tdTomato</sup> reporter line. Instead of attempting to reconcile the controversies regarding GRP expression, we focused more on utilizing the genetically labeled mouse lines to study the function of this subset of spinal cord neurons in pain and itch sensation. To further determine the laminar distribution of the *Grp*<sup>+</sup> neurons in the dorsal horn, we performed immunostaining on *Grp*<sup>Cre</sup>; *ROSA26*<sup>L<sup>SL</sup>-tdTomato</sup> spinal sections. *Grp*<sup>+</sup> neurons were located deeper than the CGRP-labeled terminals in lamina II outer layer (Figure 1E), colocalized with IB4 positive fibers in lamina II dorsal inner layer (Figure 1F), and partially overlapped with PKC $\gamma$

neurons (9.03%) in ventral inner layer (Braz et al., 2014; Solorzano et al., 2015; Figures 1G and S1E). Since there are no projection neurons (i.e., dorsal-horn neurons sending their axons to the brain) in lamina II (Todd, 2010), *Grp*<sup>Cre</sup> line thus labels a subset of interneurons (i.e., neurons whose axons remain and arborize in the spinal cord) in the lamina II inner layer. Regarding neurotransmitter types, more than 90% of *Grp*<sup>+</sup> neurons expressed the glutamatergic excitatory marker (Figures 1H and 1K) vesicular glutamate transporter (*vGlut2*); conversely, less than 10% of *Grp*<sup>+</sup> neurons overlapped with the GABAergic inhibitory marker *GAD1* (Figure 1I). Therefore, *Grp* labels a subset of excitatory interneurons in lamina II inner layer.

To check the prevalence of *Grp*<sup>+</sup> neurons in the spinal cord, we stained for pan-neuronal marker NeuN. *Grp* labeled only 4.24% of neurons in lamina II (Figure S1). Moreover, *Grp*<sup>+</sup> neurons were all characterized as vertical neurons according to morphology ( $n = 16$ ) (Grudt and Perl, 2002; Figures 1J and 1J'). Such a small group of genetically labeled neurons with uniform morphologies likely have uniform functions. Thus the *Grp*<sup>Cre</sup> line from GENSAT serves as a great tool to investigate this small subset of spinal interneurons.

GENSAT has another *Grp* line with EGFP expression under the same promoter. Of neurons from the *Grp*<sup>EGFP</sup> line, 93% were reported to express *Grp* mRNA (Solorzano et al., 2015). We crossed the EGFP line with *Grp*<sup>Cre</sup>; *ROSA26*<sup>L<sup>SL</sup>-tdTomato</sup>. 90.3% of *Grp*<sup>Cre</sup>-positive neurons also expressed *Grp*<sup>EGFP</sup> (Figures 1C and S1), while 64.1% of *Grp*<sup>EGFP</sup> neurons colocalized with *Grp*<sup>Cre</sup>, showing that the *Grp*<sup>EGFP</sup> line labeled most *Grp*<sup>Cre</sup>-positive neurons. We found that the distribution of *Grp*<sup>EGFP</sup>-labeled neurons overlapped with *MrgprA3* central terminals in the spinal cord (Figure 1D). Moreover, *Grp*<sup>EGFP</sup> colocalized with both *MrgprA3* and post-synaptic marker PSD95 (Figure S1), suggesting that *Grp*<sup>+</sup> neurons could form synaptic contacts with *MrgprA3*-labeled (diagramed in Figure 1L), itch-selective neurons in DRG (Han et al., 2013).

### *Grp*<sup>+</sup> Neurons Receive Direct Synaptic Inputs from Itch-Selective Primary Neurons

Next, to directly examine the synaptic inputs to *Grp*<sup>+</sup> neurons, we recorded from *Grp*<sup>+</sup> neurons in spinal slices while electrically stimulating the dorsal root. All *Grp*<sup>+</sup> neurons had monosynaptic input from C fibers (Figure S2), demonstrating that *Grp* exclusively labels second-order neurons with direct synaptic input from DRG. We then tried to further determine the source of C fiber inputs onto *Grp*<sup>+</sup> neurons. To determine whether *Grp*<sup>+</sup> neurons receive direct synaptic input from *MrgprA3*<sup>+</sup> neurons, we crossed *MrgprA3*<sup>Cre</sup> with Cre-dependent Channelrhodopsin reporter line *ROSA26*<sup>L<sup>SL</sup>-ChR2</sup> to selectively activate *MrgprA3* fibers with blue light (as diagramed in Figure 2A).

To test the behavioral effect of light-mediated activation of the *MrgprA3*<sup>+</sup> neurons, we shone blue light on the shaved nape regions of *MrgprA3*<sup>Cre</sup>; *ROSA26*<sup>L<sup>SL</sup>-ChR2</sup> mice (as diagramed in Figure 2A). The 1 Hz 100 ms light stimulation generated significant scratching compared with controls (Figure 2B; Movie S1). Similar to chemical activation (Han et al., 2013), optogenetic activation generated only scratching but not wiping behavior, which confirmed the role of *MrgprA3*<sup>+</sup> neurons as itch-selective neurons. The 5 Hz light stimulation, however, failed to elicit

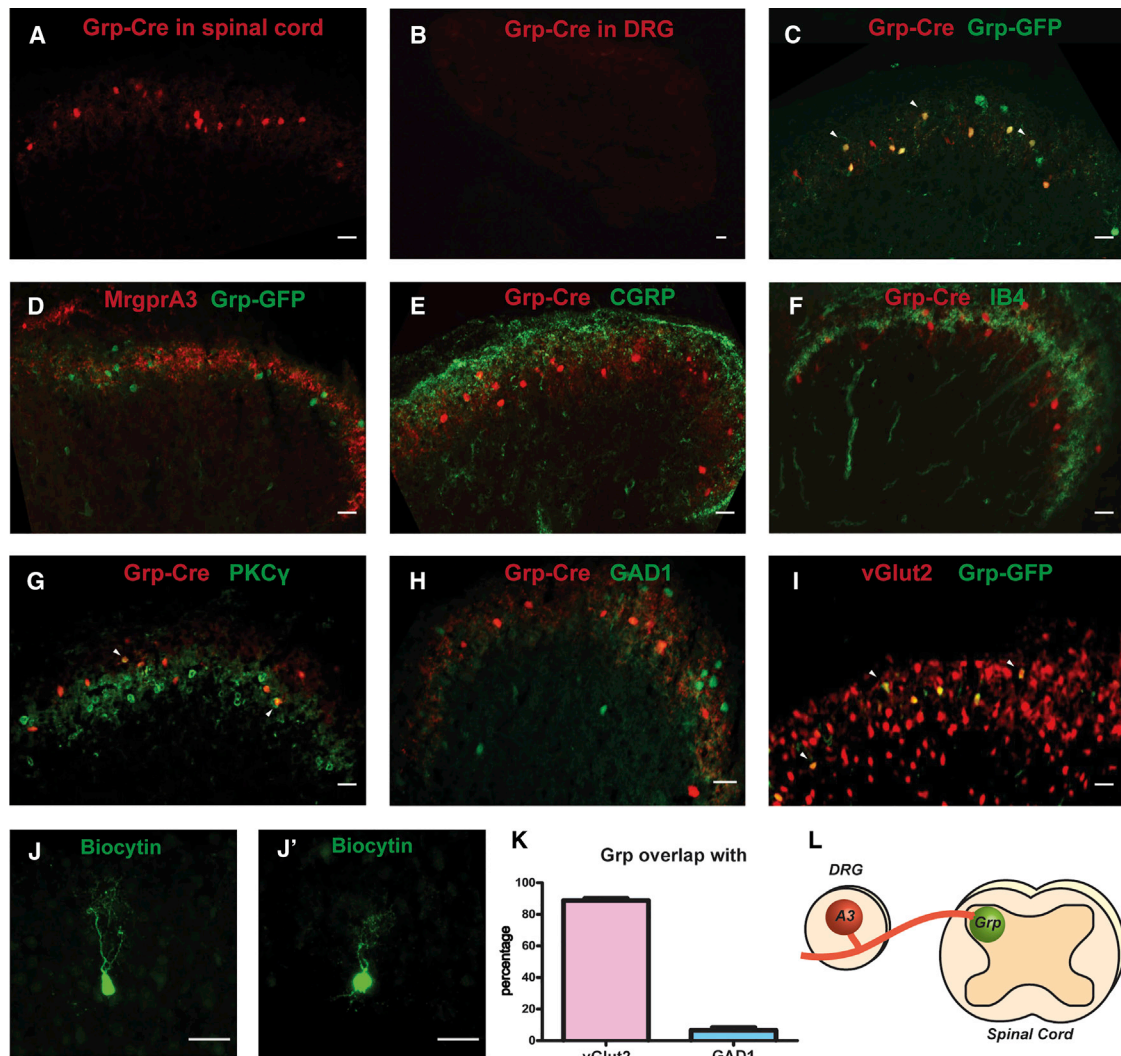


**Figure 1. Genetic Labeling of Itch Second-Order Neurons in the Spinal Cord**

(A and B) tdTomato fluorescence from (A) the spinal cord and (B) the DRG sections from *Grp<sup>Cre</sup>; ROSA26<sup>LSL-tdTomato</sup>* mice was visualized directly, without staining. (C and D) *Grp<sup>Cre</sup>; ROSA26<sup>LSL-tdTomato</sup>; Grp<sup>EGFP</sup>* (C) and *MrgprA3<sup>Cre</sup>; ROSA26<sup>LSL-tdTomato</sup>; Grp<sup>EGFP</sup>* (D) spinal sections stained with GFP antibody.

(E–G) *Grp<sup>Cre</sup>; ROSA26<sup>LSL-tdTomato</sup>* spinal sections stained with antibodies to (E) CGRP, (F) IB4, and (G) PKC $\gamma$ .

(H and I) *Grp<sup>Cre</sup>; ROSA26<sup>LSL-tdTomato</sup>; Gad1<sup>EGFP</sup>* (H) and *vGlut2<sup>Cre</sup>; ROSA26<sup>LSL-tdTomato</sup>; Grp<sup>EGFP</sup>* (I) spinal sections stained with GFP antibody. White arrowheads in (C), (G), and (I) indicate overlap.

(J and J') Individual, biocytin-labeled *Grp<sup>+</sup>* neurons, categorized as vertical neurons. All scale bars represent 20  $\mu$ m.

(K) Percentage of *Grp<sup>+</sup>* neurons expressing *vGlut2* and *Gad1*.  $n = 15$  hemisections from three mice per group. Data are represented as mean  $\pm$  SEM.

(L) Diagram summarizing the potential synaptic connections between *MrgprA3<sup>+</sup>* DRG neurons and *Grp<sup>+</sup>* neurons in the spinal cord. *MrgprA3* also overlapped with *Grp* and the postsynaptic marker PSD95.

scratching above baseline (Figure 2B, see also Figure S3C). Consistently, 1 Hz light stimulation reliably evoked action potentials in *MrgprA3<sup>+</sup>* neurons, while 5 Hz light stimulation failed to do so (Figure S3), suggesting that these neurons might not be able to fire at this higher frequency. Yet failure of 5 Hz light to induce scratching could also be caused by failure in synaptic transmission in the central synapses or central terminals to follow at this frequency.

When we recorded from the *Grp<sup>+</sup>* neurons while stimulating the *MrgprA3* central terminals with light, 100% of the *Grp<sup>+</sup>* neu-

rons (16/16) received monosynaptic input from *MrgprA3<sup>+</sup>* neurons (Figure 2C, see also Figure S3, monosynaptic connections inferred from no failure of EPSCs to 20 stimuli at 1 Hz), showing that all sampled *Grp<sup>+</sup>* neurons labeled a functionally unified population of second-order neurons that appeared to receive direct itchy input from the periphery. When we recorded from surrounding *Grp*-negative neurons, 25% of them (7/28) also received monosynaptic input, an additional 18% (5/28) received polysynaptic input, and the remaining 57% (16/28) had no connection with *MrgprA3<sup>+</sup>* neurons (Figure 2D), suggesting that

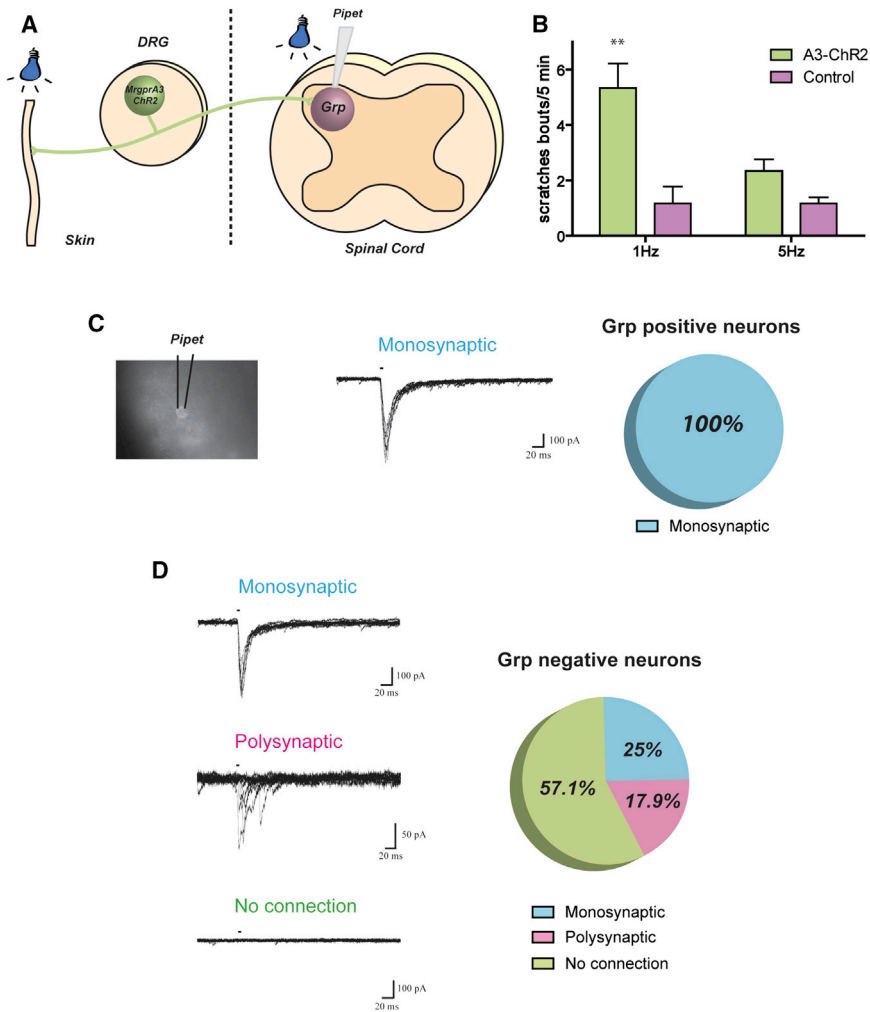


### Figure 2. *Grp*<sup>+</sup> Neurons Receive Monosynaptic Itchy Input

(A) Left: diagram showing light activation of *MrgprA3* peripheral fibers in behavioral tests; right: diagram showing light activation of *MrgprA3* central terminals and recording of *Grp*<sup>+</sup> neurons in the spinal cord.

(B) 1 Hz and 5 Hz 100 ms light stimulation triggered scratching bouts in 5 min. *MrgprA3*<sup>Cre</sup>; *ROSA26*<sup>LSL-ChR2</sup> and *ROSA26*<sup>LSL-ChR2</sup> control mice had light delivered to shaved nape regions ( $n = 6$ ). Data are represented as mean  $\pm$  SEM.

(C) From left to right: image of *Grp*<sup>+</sup> neurons in spinal slice with electrode (black lines), representative traces of light-induced EPSCs in *Grp*<sup>+</sup> neurons with monosynaptic input from *MrgprA3*<sup>+</sup> neurons, and percentage of *Grp*<sup>+</sup> neurons with monosynaptic input from *MrgprA3*<sup>+</sup> neurons.

(D) Left: representative traces of light-induced EPSCs in lamina II *Grp*-negative neurons with monosynaptic input, polysynaptic input, and no synaptic input from *MrgprA3*<sup>+</sup> neurons; right: percentage of lamina II *Grp*-negative neurons with monosynaptic input, polysynaptic input, and no synaptic input from *MrgprA3*<sup>+</sup> neurons.

*Grp* labels a subset of itch second-order neurons in the spinal cord.

### *Grp*<sup>+</sup> Neurons Receive Monosynaptic Input from Both Itch and Pain Primary Sensory Neurons

We then checked whether *Grp*<sup>+</sup> neurons receive input from nociceptors other than pruriceptors in DRG. However, it is hard to selectively activate nociceptors without also targeting the itch-selective neurons, given that they share many genetic markers. Therefore, we decided to use monosynaptic rabies tracing (Wickersham et al., 2007) to systemically quantify the inputs to the *Grp*<sup>+</sup> population. AAV helper virus (AAV8-LSL-TVA-EGFP-B19G) was injected into the spinal cord to enable expression of TVA receptor and rabies glycoprotein in Cre-expressing neurons. Deficient rabies virus ( $\Delta$ G-RV-GFP) then specifically infected TVA-expressing *Grp*<sup>+</sup> neurons, which also contained the rabies glycoprotein that allowed transsynaptic labeling (as diagrammed in Figure 3A).

Deficient rabies virus successfully infected *Grp*<sup>+</sup> neurons in spinal cord lamina II, but not in Cre-negative mice or when injected without the helper virus (Figures 3B and S4), confirming the specificity of viral tracing. In DRG, rabies virus transsynapti-

cally labeled mostly small- to medium-diameter neurons. A total of 64.1% of rabies-labeled DRG neurons expressed peptidergic marker calcitonin gene-related peptide (CGRP), and 39.3% of rabies-labeled DRG neurons expressed nonpeptidergic marker IB4, while very few (3.85%) expressed myelinated neuronal marker NF200 (Figures 3C and 3D). In addition, 50.0% of rabies-labeled neurons were positive for nociceptive marker TrpV1; an available *MrgprC11* antibody, which marks most *MrgprA3*<sup>+</sup> itch neurons (Han et al., 2013), labeled 22.3% of rabies-infected neurons, confirming that *Grp*<sup>+</sup> neurons received monosynaptic input from itch-selective neurons (Figure 3D). Since the nociceptive neuron markers CGRP, IB4, and TrpV1 (which could also be expressed in some pruriceptors) labeled a larger percentage of rabies-infected DRG neurons than the marker for itch neurons, we conclude that *Grp*<sup>+</sup> neurons received monosynaptic input from nociceptive populations in addition to itch-selective neurons.

### Painful Stimuli Strongly Activate *Grp*<sup>+</sup> Neurons, while Itchy Stimuli Weakly Activate *Grp*<sup>+</sup> Neurons

Since our results suggest that *Grp*<sup>+</sup> neurons receive direct synaptic inputs from both itch and pain primary sensory neurons, we next tried to determine whether *Grp*<sup>+</sup> neurons can distinguish between painful and itchy inputs. We performed DRG-attached spinal slice recordings and applied drugs on DRG cell bodies to mimic natural painful and itchy stimuli coming from the periphery (Figure 4A). Both pain- and itch-producing drugs applied directly on DRG triggered action potentials in *Grp*<sup>+</sup> neurons (Figures 4C–4F). Capsaicin evoked

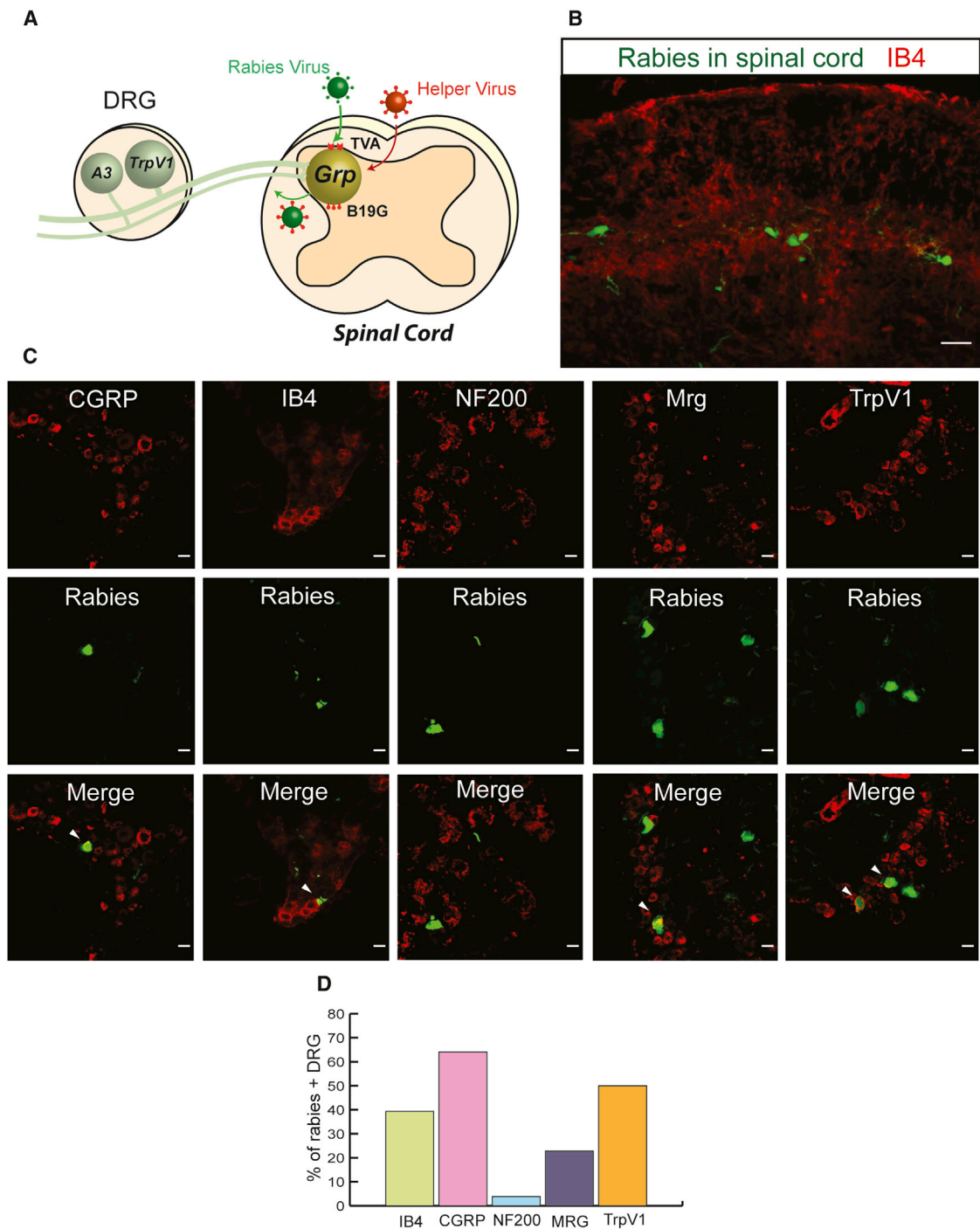


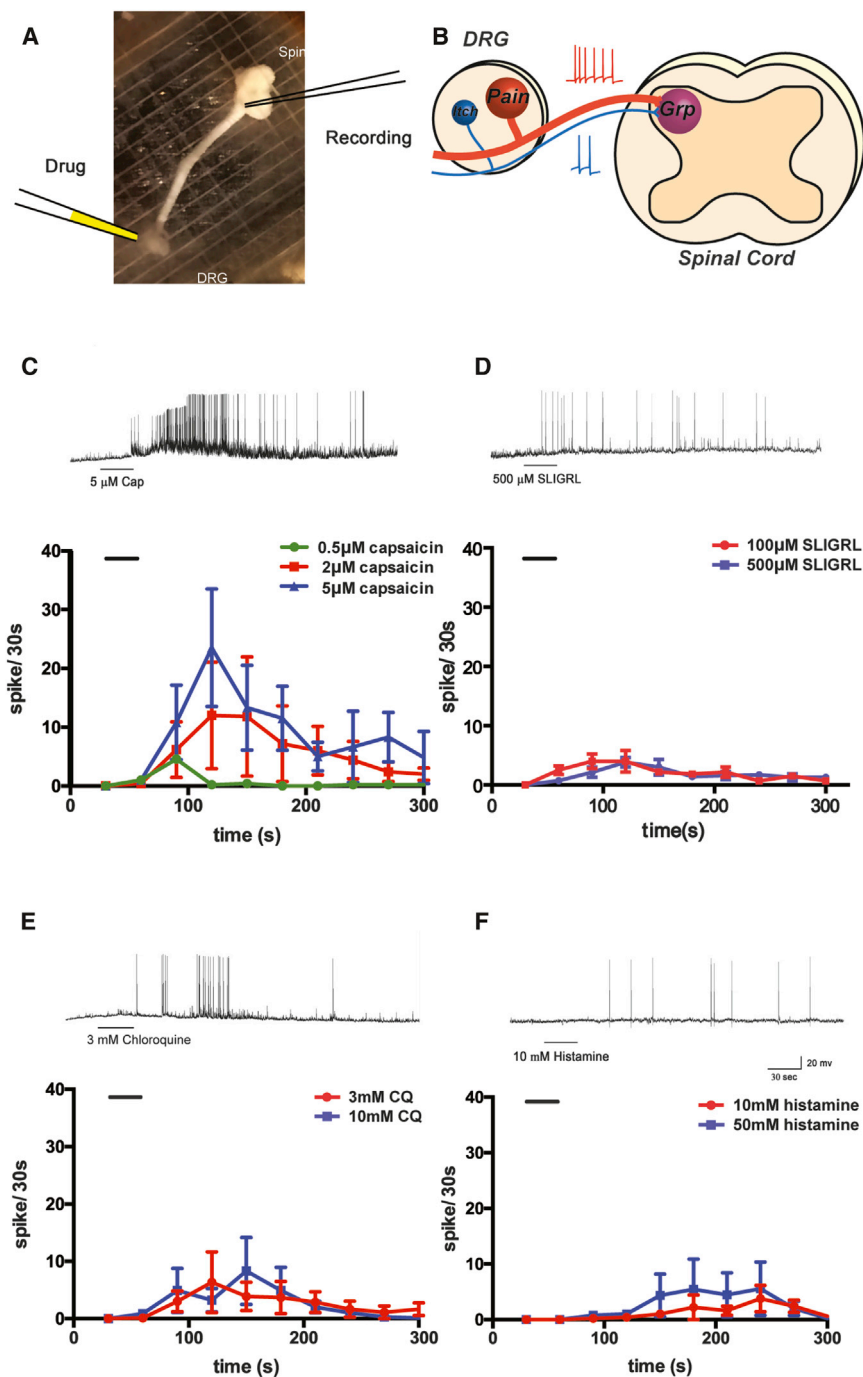
### Figure 3. Monosynaptic Retrograde Tracing from *Grp*<sup>+</sup> Neurons

(A) Diagram showing monosynaptic retrograde tracing strategy from *Grp*<sup>+</sup> neurons.

(B) Rabies-labeled neurons overlap with IB4 in spinal cord.

(C) Top: L4-6 DRG sections labeled with different markers (CGRP, IB4, NF200, MrgprC11, and TrpV1); middle: rabies virus transsynaptically labeled DRG neurons; bottom: merged images. Arrowhead indicates overlap of markers and rabies-labeled DRG neurons. All scale bars represent 20  $\mu$ m.

(D) Percentage of rabies transsynaptically labeled DRG neurons colocalized with different markers. Pooled results from more than 30 DRG sections of at least five mice for each marker.



high-frequency firing in *Grp*<sup>+</sup> neurons, while the pruritogen SLIGRL produced only weak firing on the same recorded neurons, even at very high doses. To ensure that limited penetration of peptide SLIGRL did not affect the responses of *Grp*<sup>+</sup> neurons, we applied the small-molecule pruritogens histamine and chloroquine. Similarly, histamine and chloroquine generated weaker firing in *Grp*<sup>+</sup> neurons than capsaicin ( $p < 0.001$  and  $p < 0.001$ , respectively; two-way ANOVA), which indicates that these neurons fire strongly in response to painful stimuli but

#### Figure 4. Painful Stimuli Strongly Activate *Grp*<sup>+</sup> Neurons, while Itchy Stimuli Weakly Activate *Grp*<sup>+</sup> Neurons

(A) Image of DRG-attached spinal cord slice. Recording electrode on right and drug application electrode on left.

(B) Diagram summarizing concept that painful stimuli from DRG can strongly activate *Grp*<sup>+</sup> neurons while itchy stimuli can only weakly activate *Grp*<sup>+</sup> neurons.

(C–F) Top: representative traces of action potentials from *Grp*<sup>+</sup> neurons in responses to drugs; bottom: *Grp*<sup>+</sup> neurons in response to (C) capsaicin ( $n = 5$ , 0.5  $\mu$ M;  $n = 5$ , 2  $\mu$ M;  $n = 6$ , 5  $\mu$ M), (D) SLIGRL ( $n = 7$ , 100  $\mu$ M;  $n = 6$ , 500  $\mu$ M), (E) chloroquine (CQ) ( $n = 9$ , 3 mM;  $n = 10$ , 10 mM), and (F) histamine ( $n = 5$ , 10 mM;  $n = 9$ , 50 mM) application on DRG. Black bar indicates duration of drug application ( $n = 6$ ). Data are represented as mean  $\pm$  SEM.

weakly in response to itchy stimuli (diagrammed in Figure 4B). Consistent with our results, several previous studies showed that spinal interneurons and projection neurons fired at higher frequencies in response to painful stimuli than in response to itchy stimuli (Akiyama et al., 2009b; Davidson et al., 2007,2012).

#### Coding of Both Pain and Itch by *Grp*<sup>+</sup> Neurons

Although the itch neurons in DRG are responsive to both painful and itchy stimuli, activation of these neurons generates itch and not pain responses (Han et al., 2013). Similarly, *Grp*<sup>+</sup> neurons appear to receive direct synaptic input from both pain and itch primary neurons. Using behavioral assays, we next determined what sensations are generated by the activation of *Grp*<sup>+</sup> neurons. To specifically activate *Grp*<sup>+</sup> neurons, we crossed *Grp*<sup>Cre</sup> line to cre-dependent reporter line *ROSA26*<sup>LSL-TrpV1</sup> in a global TrpV1 knockout background (*Grp*<sup>Cre</sup>; *ROSA26*<sup>LSL-TrpV1</sup>; *TrpV1*<sup>-/-</sup>). In *Grp*<sup>Cre</sup>; *ROSA26*<sup>LSL-TrpV1</sup>; *TrpV1*<sup>-/-</sup> mice, *Grp*<sup>+</sup> neurons were the only cells with TrpV1

expression (as diagrammed in Figure 5A); therefore, TrpV1 agonist capsaicin can selectively activate *Grp*<sup>+</sup> neurons. To test the functional expression of TrpV1, we injected AAV1-LSL-TdTomato virus into the spinal cord and recorded from tdTomato-labeled *Grp*<sup>+</sup> neurons. Labeled neurons from *Grp*<sup>Cre</sup>; *ROSA26*<sup>LSL-TrpV1</sup>; *TrpV1*<sup>-/-</sup> mice, but not from *Grp*<sup>Cre</sup>; *TrpV1*<sup>-/-</sup> mice, responded to capsaicin (Figure S5). *Grp*<sup>+</sup> neurons with ectopic TrpV1 expression showed lower sensitivity to capsaicin than did TrpV1<sup>+</sup> DRG neurons. These neurons exhibited monotonically

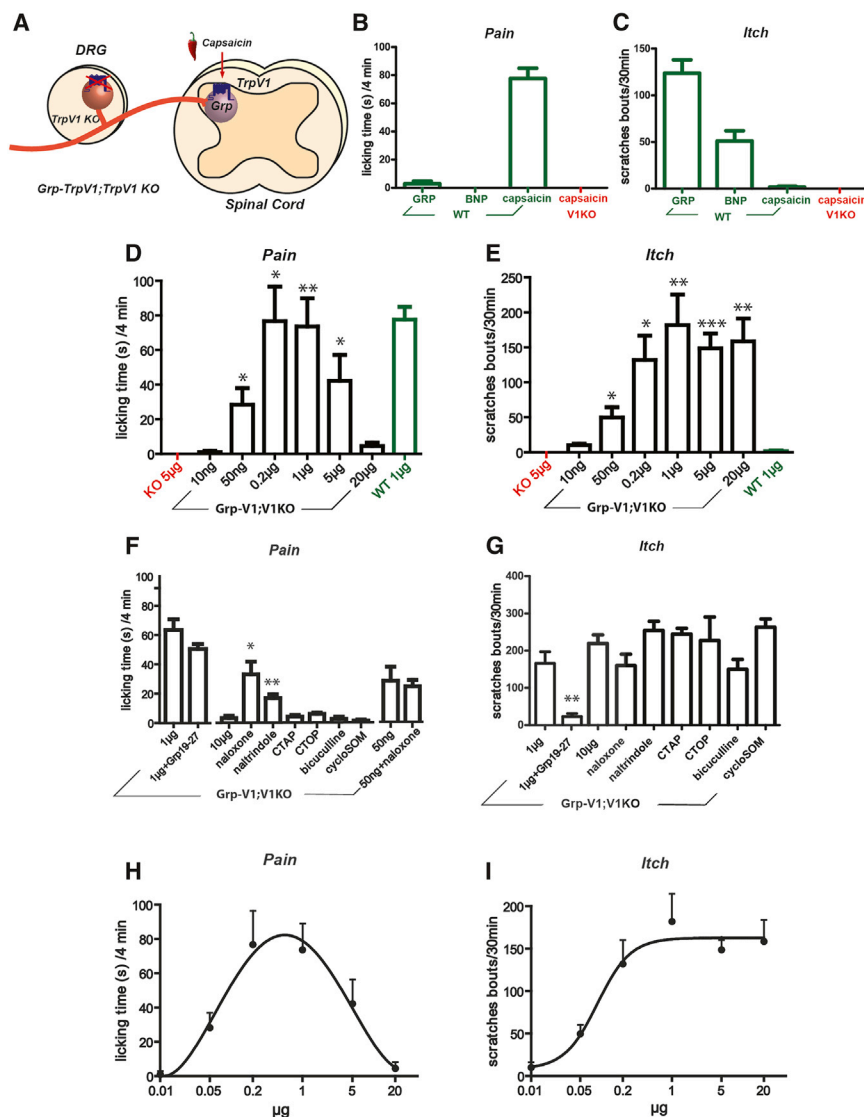


**Figure 5. Intensity-Dependent Coding of Pain and Itch by *Grp*<sup>+</sup> Neurons**

(A) Diagram showing the strategy of capsaicin-mediated specific activation of *Grp*<sup>+</sup> neurons in *Grp*<sup>Cre</sup>; *ROSA26*<sup>LSL-TrpV1</sup>; *TrpV1*<sup>-/-</sup> mice.

(B and C) Pain-related licking time (B) and itch-related scratching bouts (C) in wild-type (green bars) and *TrpV1*<sup>-/-</sup> (red bars) mice triggered by intrathecal delivery of 10  $\mu$ L capsaicin (1  $\mu$ g or 3.3 nmol,  $n = 6$  for both genotypes), BNP (2.5 mg/mL or 7.1 nmol/site,  $n = 8$ ), and GRP peptides (200  $\mu$ M or 2 nmol/site,  $n = 8$ ).

(D and E) 10  $\mu$ L intrathecal capsaicin-triggered pain (D) and itch (E) responses in *Grp*<sup>Cre</sup>; *ROSA26*<sup>LSL-TrpV1</sup>; *TrpV1*<sup>-/-</sup> mice (black bars, from left to right: 10 ng or 0.03 nmol,  $n = 9$ ; 50 ng or 0.16 nmol,  $n = 6$ ; 0.2  $\mu$ g or 0.67 nmol,  $n = 5$ ; 1  $\mu$ g or 3.33 nmol,  $n = 6$ ; 5  $\mu$ g or 16.7 nmol,  $n = 10$ ; 20  $\mu$ g or 66.7 nmol,  $n = 6$ ) together with responses in wild-type (green bars, 1  $\mu$ g or 3.33 nmol,  $n = 6$ ) and *TrpV1*<sup>-/-</sup> (red bars, 5  $\mu$ g or 16.7 nmol,  $n = 6$ ) mice from (B) and (C).

(F and G) 10  $\mu$ L intrathecal capsaicin-triggered pain (F) and itch (G) responses in *Grp*<sup>Cre</sup>; *ROSA26*<sup>LSL-TrpV1</sup>; *TrpV1*<sup>-/-</sup> mice with drugs. From left to right: 1  $\mu$ g or 3.33 nmol capsaicin without and with 200  $\mu$ M or 2 nmol/site GRPR antagonist Deamino-Phe<sup>19</sup>, D-Ala<sup>24</sup>, D-Pro<sup>26</sup>, psi(CH<sub>2</sub>NH)Phe<sup>27</sup>-GRP (19–27) ( $n = 6$  and 5); 10  $\mu$ g or 33.3 nmol capsaicin with naloxone (1  $\mu$ g or 3.33 nmol,  $n = 7$ ), naltrindole (10  $\mu$ g or 24.1 nmol,  $n = 7$ ), CTAP (5  $\mu$ g or 13.7 nmol,  $n = 6$ ), CTOP (10  $\mu$ g or 9.43 nmol,  $n = 6$ ), bicuculline (10  $\mu$ M or 0.1 nmol,  $n = 7$ ), cyclosomatostatin (0.1 mM or 1 nmol,  $n = 8$ ), and for (F) 5  $\mu$ g/mL or 0.16 nmol capsaicin without ( $n = 6$ ) and with naloxone (1  $\mu$ g or 3.33 nmol,  $n = 9$ ).

(H and I) Pain (H) and itch (I) dose-response curve fitting of (D) and (E). Data are represented as mean  $\pm$  SEM. \*,  $p < 0.05$ ; \*\*,  $p < 0.01$ ; \*\*\*,  $p < 0.001$ ; two-tailed unpaired Student's *t* test. Abbreviations are as follows: WT, short for wild-type; KO, short for *TrpV1*<sup>-/-</sup>; Grp-V1;V1KO, short for *Grp*<sup>Cre</sup>; *ROSA26*<sup>LSL-TrpV1</sup>; *TrpV1*<sup>-/-</sup>.

increased responses to a wide range of capsaicin doses (Figure S5), confirming the functional expression of *TrpV1* in *Grp*<sup>+</sup> neurons.

Drugs known to produce pain (capsaicin) and itch (gastrin-releasing peptide, GRP, and brain natriuretic peptide, BNP) were first tested intrathecally in wild-type mice. Previous studies reported mixed licking, biting, and scratching responses to capsaicin (Hunnskaar et al., 1985; Yaksh et al., 1979). Counting licking and biting together separately from scratching revealed that responses in mice were predominantly licking and biting, with very few bouts of scratching (Hunnskaar et al., 1986). To further distinguish licking, indicating pain, and biting, indicating itch, behaviors were recorded with a high-definition camera and four side mirrors to enable views from all angles (Figure S5; LaMotte et al., 2011). When played back at 1/4 normal speed, licking but not biting responses were detected following injections of

capsaicin. Short-lasting licking responses (<5 min) directed to the lower back regions were predominantly observed at a characteristic frequency of 5 Hz and were accompanied by minor scratching responses, as previously reported (Figure 5B). Such responses were not seen in *TrpV1*<sup>-/-</sup> mice, ensuring specificity. GRP and BNP nonetheless produced scratching that lasted about 30 min after injection and minor licking responses (Figures 5C and S5B).

Surprisingly, specific activation of *Grp*<sup>+</sup> neurons in *Grp*<sup>Cre</sup>; *ROSA26*<sup>LSL-TrpV1</sup>; *TrpV1*<sup>-/-</sup> mice by intrathecal injection of capsaicin generated both pain-related licking and itch-related scratching (Movie S2), whereas injection of capsaicin generated no response in Cre-negative control mice (*ROSA26*<sup>LSL-TrpV1</sup>; *TrpV1*<sup>-/-</sup>) and only pain-related licking in wild-type mice (Figures 5B and 5C), which confirms the specificity of the activation responses. The licking responses lasted only about 4 min after injection (similar to the licking responses in wild-type mice) and

were not affected by intrathecal injection of a GRPR antagonist (Figure 5F). The scratching responses lasted more than 30 min and were effectively blocked by GRPR antagonist (Figure 5G); this is consistent with the critical role of GRPR neurons in itch transmission (Sun et al., 2009; Sun and Chen, 2007). Thus, the activation of *Grp*<sup>+</sup> neurons can trigger both robust pain and itch responses, a phenomenon rarely observed. *Grp*<sup>+</sup> neurons appear to receive monosynaptic inputs from both itch and pain neurons and to code for both itch and pain, showing unexpected convergence of two related sensations in the spinal cord.

### Intensity-Dependent Coding of Pain by *Grp*<sup>+</sup> Neurons

Next, we examined the relationship between neuronal activation and behavior by determining the behavioral effects of various doses of capsaicin. Itch responses monotonically increased until a plateau was reached and were fitted to the Hill equation ( $R^2 = 0.97$ , Figures 5E and 5I). Pain responses, surprisingly, showed an inverted U relationship (Figure 5D). Increased amounts of capsaicin resulted in increased licking time that peaked and then decreased with higher capsaicin doses; weak and strong activation produced little pain behavior while medium range activation generated the greatest pain responses. Not surprisingly, pain dose responses were fitted well with a polynomial equation ( $R^2 = 0.99$ , Figure 5H). Given that high doses of capsaicin still caused robust itch responses, the inverted U pain responses were unlikely to be caused by desensitization. Thus, *Grp*<sup>+</sup> neurons demonstrate intensity-dependent coding. Rather than generating itch sensation with weak activation and pain sensation with strong activation, as suggested by the original intensity theory, *Grp*<sup>+</sup> neurons monotonically code for itch while pain is coded only by inputs of medium intensities.

We reasoned that the inverted U coding of pain could be generated by a combination of direct coding effects and another pain inhibition circuit. To uncover this pain inhibition mechanism, we attempted to “rescue” pain responses during strong activation of the *Grp*<sup>+</sup> neurons. An opioid antagonist, naloxone, at a dose not eliciting pain itself, “rescued” the pain responses from almost zero to about half of the maximal level. Both bicuculline, a GABA A antagonist, and cyclo-somatostatin, the antagonist of antinociceptive somatostatin highly expressed in the surrounding region, failed to “rescue” the pain responses (Figure 5F). Successfully rescuing pain responses again confirmed that *Grp*<sup>+</sup> neurons were not desensitized by high doses of capsaicin. To demonstrate that naloxone was not simply blocking the basal activity of the endogenous opioid system independent of *Grp* activation, we coinjected naloxone with a low dose of capsaicin, which can produce both medium pain and itch responses. No effect was observed on pain responses (Figure 5F), indicating that the endogenous opioid system was only recruited to inhibit pain during strong activation of the *Grp*<sup>+</sup> neurons. Thus, the endogenous opioid system is at least partially responsible for the pain inhibition associated with strong activation of the *Grp*<sup>+</sup> neurons and therefore, together with direct pain coding by the *Grp*<sup>+</sup> neurons, generates this inverted U response curve.

We then determined which endogenous opioid peptide was employed to block pain by utilizing the mu opioid antagonists CTAP and CTOP and the delta opioid antagonist naltrindole.

Naltrindole, but not CTAP or CTOP, induced a similar rescue effect as naloxone (Figure 5F), while none of the drugs affected itch responses (Figure 5G). These results suggest that enkephalin, the endogenous ligand for delta opioid receptors, was recruited by *Grp*<sup>+</sup> neurons to inhibit pain, but not itch, which is consistent with previously reported enkephalin effects (Lee and Ko, 2015). On the contrary, another endogenous opioid, dynorphin, was reported to inhibit itch, but not pain (Kardon et al., 2014). Colocalization of *Grp*, enkephalin, and synaptic marker PSD95 also suggests that enkephalin-expressing interneurons may be synaptically connected to *Grp*<sup>+</sup> neurons (Figure S5). To directly test this, we utilized *Penk*<sup>Cre</sup> line to label enkephalin-expressing neurons in the spinal cord and verified the expression of enkephalin in these inhibitory interneurons (Figures 6D and 6E), as previously reported (Fukushima et al., 2011; Todd et al., 1992). Patch-clamped recordings of *Grp*<sup>EGFP</sup> neurons were made in spinal cord slices from *Grp*<sup>EGFP</sup>; *Penk*<sup>Cre</sup>; *ROSA26*<sup>LSL-GCaMP6</sup> mice. Depolarization of a single *Grp*<sup>EGFP</sup> neuron triggered activation of enkephalin-expressing neurons, as monitored by GCaMP6 calcium imaging, in 50% of cases (five out of ten neurons, Figure 6C), confirming the synaptic connections between *Grp*<sup>+</sup> neurons and enkephalin-expressing neurons. This percentage may be an underestimate, since some connections might be lost during sectioning. In addition, enkephalin release was detected by ELISA when *Grp*<sup>Cre</sup>; *ROSA26*<sup>LSL-TrpV1</sup>; *TrpV1*<sup>-/-</sup> spinal cords were treated with high-dose capsaicin, but not when they were treated with low-dose or no capsaicin (Figure 6B). Furthermore, spinal cords from Cre-negative control mice (*ROSA26*<sup>LSL-TrpV1</sup>; *TrpV1*<sup>-/-</sup>) treated with high-dose capsaicin released a minimal amount of enkephalin, which confirms that the release of enkephalin is dependent on strong activation of the *Grp*<sup>+</sup> neurons. Moreover, enkephalin requires strong depolarization for release (Cesselin et al., 1984; Neuman et al., 1984), consistent with the observation that only strong activation of the *Grp*<sup>+</sup> neurons triggers pain inhibition.

### *Grp*<sup>+</sup> Neurons Form Leaky Gate to Negatively Regulate Pain Transmission

Activation of the *Grp*<sup>+</sup> neuron population codes for pain but also inhibits pain through the release of enkephalin, which forms a type I incoherent feedforward loop (FFL) (summarized in Figure 7B) featuring non-monotonic output (Alon, 2007; Milo et al., 2002). An example of a pain-related type I incoherent FFL can be found in the gate control theory (Braz et al., 2014; Duan et al., 2014; Melzack and Wall, 1965; Wall, 1978). The gate control theory of pain proposes that nociceptive transmission neurons (T) receive both noxious input from C fibers and non-noxious input from A $\beta$  fibers. A $\beta$  input also indirectly inhibits nociceptive transmission neurons through inhibitory interneurons (IN), thus forming a type I incoherent FFL that can close the gate (T) and suppress painful input (Figure 7A). The somatostatin- and dynorphin-expressing interneurons have recently been implicated as transmission neurons and inhibitory interneurons, respectively, in the gate control theory (Duan et al., 2014).

Here, we present a model to explain our experimental observations and then provide more data to support the model. In the same way as A $\beta$  fibers in the gate control theory, we propose that *Grp*<sup>+</sup> neurons utilize the type I incoherent FFL

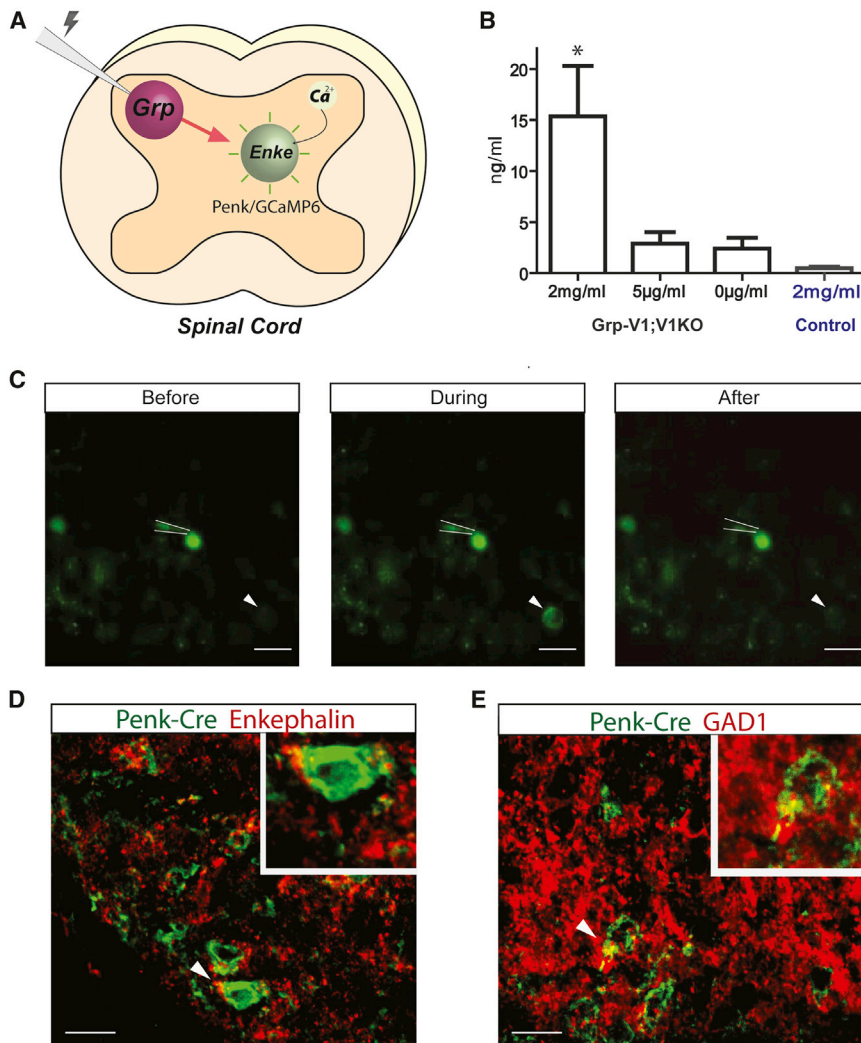


**Figure 6. Activation of Enkephalin-Expressing Neurons Triggered by Stimulation of *Grp*<sup>+</sup> Neurons**

(A) Diagram showing calcium imaging of enkephalin-expressing neurons labeled by *Penk*<sup>Cre</sup> while depolarizing *Grp*<sup>EGFP</sup> neurons in spinal slices.

(B) Enkephalin release with different doses of capsaicin from *Grp*<sup>Cre</sup>; *ROSA26*<sup>LSL-TrpV1</sup>; *TrpV1*<sup>-/-</sup> mice (black bars) and *ROSA26*<sup>LSL-TrpV1</sup>; *TrpV1*<sup>-/-</sup> control mice (blue bars) normalized to per g tissue used in ELISA. Data are represented as mean ± SEM.

(C) Representative calcium imaging results showing enkephalin-expressing neurons before, during, and after activation of *Grp*<sup>EGFP</sup> neurons (1 Hz 50 pA current injection). White lines (in pipette shape) indicate patch-clamped *Grp*<sup>EGFP</sup> neurons. Arrowheads indicate activated enkephalin-expressing neurons during *Grp* activation. Enkephalin-expressing neurons (*Penk*<sup>Cre</sup>; *Rosa26*<sup>LSL-GCaMP6</sup>) were activated when five out of ten *Grp*<sup>+</sup> neurons were depolarized.

(D) *Penk*<sup>Cre</sup> labeled neurons colocalized with enkephalin and GAD1. Representative neurons magnified in upper right corner (Arrowheads indicate magnified cells). Scale bars represent 20 µm.

as a gate to regulate pain transmission. When strongly activated, *Grp*<sup>+</sup> neurons can trigger enkephalin release to close the gate to painful signals both from *Grp*<sup>+</sup> neurons and potentially from other pain-sensing neurons in the spinal cord, resulting in reduced pain sensation (summarized in Figure 7B). However, the A $\beta$  and *Grp* gates have some fundamental differences. The A $\beta$  FFL does not let any signals through the gate, at least under physiological conditions, so that non-noxious input does not elicit pain sensations; the *Grp* FFL allows weak pain signals to pass through the gate but suppresses strong pain signals. Therefore, we named it a “leaky” gate. We think the advantage of this leaky gate is that passing on weak signals ensures sensitivity to weak painful stimuli, while inhibiting strong signals prevents overwhelming pain sensations.

#### Increased Pain and Decreased Itch after Ablation of *Grp*<sup>+</sup> Neurons

According to our leaky gate model, the *Grp* FFL functions as a “brake” to prevent strong pain signals from overwhelming the

system. Therefore, we predicted that the loss of the *Grp*<sup>+</sup> neurons should lead to an increase in pain responses. To directly test this prediction, we ablated *Grp*<sup>+</sup> neurons with diphtheria toxin. Diphtheria toxin receptors (DTRs) were specifically expressed in *Grp*<sup>+</sup> neurons with Cre-dependent *ROSA26*<sup>LSL-DTR</sup> line together with *ROSA26*<sup>LSL-tdTomato</sup> allele to monitor ablation efficacy (Figure 8A). Diphtheria toxin treatments successfully ablated more than 95% of the *Grp*<sup>+</sup> neurons (Figures 8B and 8C). Cre-negative mice (*ROSA26*<sup>LSL-DTR/LSL-tdTomato</sup>) treated with same doses of diphtheria toxin were used as controls. Ablated mice were healthy and had normal motor coordination in the rotarod test (Figure S6). In addition, CGRP- and IB4-labeled lamina II regions showed no change after ablation, indicating that the loss of such a small population did not obviously affect the general organization of the local circuitries. The number of PKC $\gamma$ -positive neurons was reduced, consistent with the partial overlap between PKC $\gamma$  and *Grp*<sup>+</sup> neurons, while the number of Pax2<sup>+</sup> interneurons was comparable between ablated and control mice, confirming that diphtheria toxin treatment did not produce nonspecific neurotoxicity (Figure S6).

First, we tested acute pain responses. Pain behavioral responses induced by injection of capsaicin into both the cheek and intraplantar surface of the hindpaw greatly increased after ablation (Figure 8E, yellow shaded). *Grp*<sup>Cre</sup>; *ROSA26*<sup>LSL-DTR/LSL-tdTomato</sup> mice also had significantly shorter response latencies in all thermal pain assays, including hot plate, Hargreave, and tail immersion than control mice (Figures 8E and

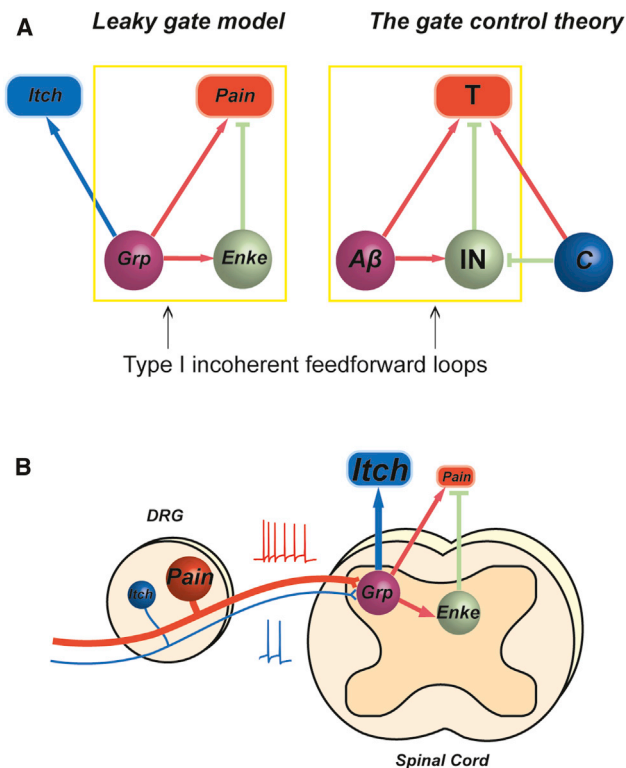


**Figure 7. "Leaky Gate" Model in Pain and Itch Transmission**

(A) Comparison of "leaky gate" model (left) and the gate control theory (right).  $Grp^+$  neurons directly code for pain and itch while inhibiting pain through enkephalin-expressing interneurons.  $A\beta$  fibers activate pain transmission neurons and also indirectly inhibit pain transmission neurons via inhibitory interneurons. Yellow rectangles indicate type I incoherent FFLs formed by  $Grp^+$  neurons and  $A\beta$  fibers, respectively.

(B) Diagram summarizing the role of  $Grp^+$  neurons in pain and itch coding.  $Grp^+$  neurons receive weak input from itchy stimuli and strong input from painful stimuli, and they positively code for itch while negatively regulating pain transmission. Enke represents enkephalin, T represents pain transmission neurons, and IN represents inhibitory interneurons.

8F). Mechanical sensitivity tested by Von Frey filaments remained the same in both genotypes (Figure 8G). Thus, the loss of  $Grp^+$  neurons enhanced chemical and thermal pain as predicted by the leaky gate model. We next examined itch responses. Scratching responses to multiple pruritogens including histamine (100 mM or 5  $\mu$ M/site), chloroquine (CQ, 4 mM or 200 nmol/site), SLIGRL (1 mM or 50 nmol/site), and serotonin (5-HT, 1 mM or 50 nmol/site) were all significantly reduced in  $Grp^{Cre}; ROSA26^{LSL-DTR/LSL-tdTomato}$  mice, confirming the critical role of  $Grp^+$  neurons in itch coding (Figure 8D). Interestingly, GRPR antagonist significantly blocked histamine- and chloroquine-induced itch in control mice but did not further reduce scratching responses in  $Grp$ -neuron-ablated mice. This suggests that the residual itch responses after  $Grp$  neuron ablation are mediated by a GRPR-independent pathway (Figure 8E).

### Strong Pain Responses Are More Affected by the Loss of $Grp^+$ Neurons

Unlike in the gate control theory, only strong activation of the  $Grp^+$  neurons closes the leaky gate to inhibit pain. Therefore, the leaky

gate model predicts that weak painful stimuli might trigger less or no inhibition. Accordingly, we compared chemical pain responses (capsaicin-induced cheek wiping) with two different doses. High-dose capsaicin (1 mg/mL) produced significantly more cheek wiping in ablated mice (Figure 8E, yellow shaded), while low-dose capsaicin (0.5 mg/mL) generated similar amounts of wiping in both ablated and control mice (Figure 8F), matching our prediction that weak pain triggers no inhibition from the  $Grp$  FFL. Similarly, intraplantar injection of high-dose capsaicin (0.1 mg/mL) induced significantly more licking and flinching responses, indicating pain, in ablated animals, while low dose (0.05 mg/mL) triggered comparable responses. We also tested thermal pain using both hot plate and tail immersion, with two temperatures. Ablated mice showed reduced response latencies at both temperatures (Figures 8G and 8H). Therefore, we compared the ratios of ablated responses to control responses at the two temperatures, with a lower ratio meaning a larger increase in pain response after ablation. The ratios at high temperature were significantly lower than the ratios at low temperature in both tests, suggesting that thermal stimuli at higher temperatures resulted in larger increase in pain response after the loss of  $Grp^+$  neurons, consistent with the leaky gate model.

We also compared dose effect on itch responses, which are normally coded by the  $Grp^+$  neurons, between control and ablated mice. Ablated mice showed reduced itch responses to low doses of SLIGRL and CQ (Figure 8D), while high doses generated similar responses in both ablated and control mice (Figure S6). Thus, in contrast to pain, stronger itch responses are less affected by the loss of  $Grp^+$  neurons, potentially due to saturation or compensation from other itch second-order neurons. These results confirm that the  $Grp$  FFL has distinct roles in pain and itch coding.

## DISCUSSION

The selectivity theory depicts pain and itch coding in the spinal cord as the continuation of separate labeled lines from periphery, with pain inhibiting itch through B5-I interneurons (Kardon et al., 2014) and NPY interneurons (Bourane et al., 2015). Here, we present experimental observations and a new "leaky gate" model to expand the current coding theory of pain and itch. In combination with selectivity theory, the leaky gate model can provide better descriptions of pain- and itch-related phenomena. The data show that a subset of second-order neurons with uniform morphologies, the  $Grp^+$  population, participates in the coding of both pain and itch sensations; this potentially represents the currently underappreciated crosstalk of different sensations in the spinal cord. Another feature of the  $Grp^+$  population is the intensity-dependent coding of pain. The  $Grp^+$  neurons directly code for pain sensation and, upon strong activation, indirectly inhibit pain via the recruitment of the endogenous opioid system. The classic intensity theory suggests that pain and itch sensations are differentially coded by strong and weak activation intensities. Here, we propose that the intensity-dependent pain coding by  $Grp^+$  neurons is a form of negative regulation of pain in the spinal cord. This novel intensity-dependent coding serves as a good example of the currently overlooked non-monotonic signal processing in spinal circuits.

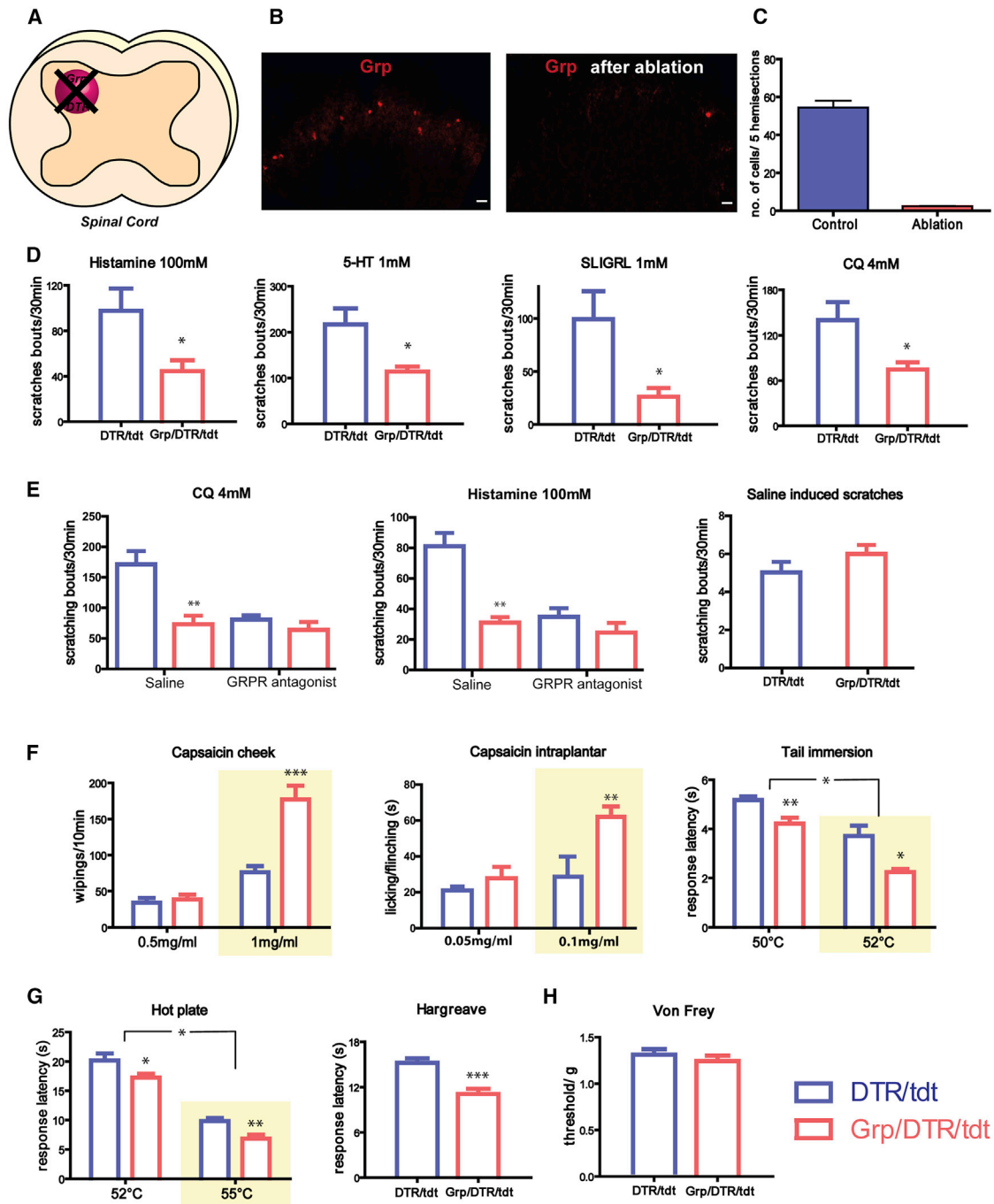


**Figure 8. Increased Pain and Decreased Itch Responses after the Ablation of *Grp*<sup>+</sup> Neurons**

(A) Diagram showing ablation of *Grp*<sup>+</sup> neurons in the spinal cord.  
 (B) Representative images of *Grp*<sup>Cre</sup>; *ROSA26*<sup>L<sup>SL-DTR</sup></sup>; *L<sup>SL-tdTomato</sup>* spinal slices with and without diphtheria toxin treatments. All scale bars represent 20  $\mu$ m.  
 (C) Quantification of *Grp*<sup>+</sup> neurons per five 20- $\mu$ m hemisections in *Grp*<sup>Cre</sup>; *ROSA26*<sup>L<sup>SL-DTR</sup></sup>; *L<sup>SL-tdTomato</sup>* (red) and *ROSA26*<sup>L<sup>SL-DTR</sup></sup>; *L<sup>SL-tdTomato</sup>* control (blue) mice after diphtheria toxin treatments (n = 5 mice).  
 (D) Scratching bouts induced by histamine (100 mM or 5  $\mu$ M, n = 6 versus 8), serotonin (1 mM or 50 nM, n = 7 versus 8), SLIGRL (1 mM or 50 nM, n = 7), and chloroquine (4 mM or 200 nM, n = 11 versus 9) injection (50  $\mu$ l) in the nape region in *Grp*<sup>Cre</sup>; *ROSA26*<sup>L<sup>SL-DTR</sup></sup>; *L<sup>SL-tdTomato</sup>* (red) and *ROSA26*<sup>L<sup>SL-DTR</sup></sup>; *L<sup>SL-tdTomato</sup>* control (blue) mice.  
 (E) Scratching bouts induced by injections of histamine (100 mM or 5  $\mu$ M, n = 6) and chloroquine (4 mM or 200 nM, n = 6) in the nape region (50  $\mu$ l) with saline (50  $\mu$ l) or GRPR antagonist (50  $\mu$ l) Deamino-Phe<sup>19</sup>,D-Ala<sup>24</sup>,D-Pro<sup>26</sup>,psi(CH<sub>2</sub>NH)Phe<sup>27</sup>-GRP (19–27) (200  $\mu$ M or 2 nM per site) pretreatments 10 min before injection and (50  $\mu$ l) saline-induced scratching bouts (n = 6) in *Grp*<sup>Cre</sup>; *ROSA26*<sup>L<sup>SL-DTR</sup></sup>; *L<sup>SL-tdTomato</sup>* (red) and *ROSA26*<sup>L<sup>SL-DTR</sup></sup>; *L<sup>SL-tdTomato</sup>* control mice (blue).  
 (F) Wiping responses to capsaicin (0.5 mg/ml and 1 mg/ml) on the cheek and licking/flinching to capsaicin (0.05 mg/ml and 0.1 mg/ml) on the plantar surface.  
 (G) Hot plate and Hargreave tests.  
 (H) Von Frey test.

(legend continued on next page)

Consistent with the intensity-dependent coding of *Grp*<sup>+</sup> neurons, we observed dose-dependent behavioral changes after the loss of *Grp*<sup>+</sup> neurons (Figures 8 and S6), suggesting that testing of multiple doses in behavioral assays could help to identify currently overlooked nonlinearity in pain and itch coding. Notably, the drug doses utilized in pain and itch behavioral tests in our study, and in the pain and itch field, were high compared with cellular studies. The specificities of these responses were largely established by previous work with respective pruritogen receptor knockouts (Han et al., 2006; Liu et al., 2009, 2011). However, receptor knockouts usually reduce, but not abolish, scratching responses, suggesting potential nonspecific effects associated with high doses in behavioral tests. The number of activated neurons or ligand-bound receptors needed to trigger behavior responses remains an open question in the field. Yet the higher doses used in behavioral tests compared with cellular assays could be at least partially explained by dilution, tissue penetration, and the differential receptor densities between nerve terminals and cell bodies. In addition, human psychophysical studies, in which subjects can orally report sensations, usually require lower doses (LaMotte et al., 2011; Sikand et al., 2011b) than animal behavioral assays, indicating the relative low sensitivity of animal behavioral tests.

*Grp*<sup>+</sup> neurons appear to receive monosynaptic input from both pain- and itch-sensing primary populations, yet painful stimuli strongly activate *Grp*<sup>+</sup> neurons while itchy stimuli weakly activate them. The weaker, pruritogen-mediated activation of *Grp*<sup>+</sup> neurons could be due to factors including the weak activation of DRG neurons by itchy stimuli, weak synaptic connections, or a small percentage of itch-responsive primary neurons. This weak activation by itchy stimuli is consistent with the failure to detect chloroquine-induced *c-fos* activity in *Grp*<sup>+</sup> neurons (Bell et al., 2016). Yet unlike enkephalin-expressing inhibitory interneurons, which require strong depolarization to release neuropeptides, the weak activation of *Grp*<sup>+</sup> neurons by pruritogens seems sufficient to trigger GRP release from these excitatory interneurons. In addition to *Grp*<sup>+</sup> neurons, some lamina II interneurons may receive monosynaptic itchy input. In lamina I, projection neurons and GRPR<sup>+</sup> interneurons might also receive direct itchy input, warranting future research to further dissect related spinal cord circuits.

Pain detection systems need to be sensitive enough to protect the body from potential harm, but when exposed to strong painful stimuli, high sensitivity may generate too much pain and interfere with proper behavioral responses. Thus, brakes are necessary. Brakes triggered by signals from A $\beta$  mechanosensitive fibers make gentle rubbing an effective way to relieve pain. The *Grp* FFL also functions as a brake for pain generated by *Grp*<sup>+</sup> population and parallel pain pathways. It positively codes for pain and

triggers enkephalin release only in response to strong activation, which is consistent with dependence of enkephalin release on strong depolarization. This prominent enkephalin-mediated pain inhibition can completely block pain responses from the *Grp*<sup>+</sup> population and further reduce pain coded by parallel pain pathways in the spinal cord; thus, its high triggering threshold ensures sensitivity to weak painful input. Meanwhile, the pain inhibition mediated by *Grp* FFL cannot be triggered by itch because itch stimuli only weakly activate *Grp*<sup>+</sup> neurons, consistent with the fact that itch can rarely inhibit pain.

The ablation experiments showed that stronger pain responses had larger increases after the ablation of the *Grp*<sup>+</sup> neurons, suggesting that the *Grp* FFL provides stronger inhibition on stronger painful input in physiological conditions, as predicted by the leaky gate model. Theoretically, weak enough painful stimuli would be positively coded by *Grp*<sup>+</sup> neurons without triggering pain inhibition. Thus, these pain responses might be weaker after the ablation of *Grp*<sup>+</sup> neurons. However, given that the *Grp*<sup>+</sup> neurons only represent a subset of pain-responsive neurons in the spinal cord, the loss of these neurons may generate a more subtle change in behavior when compared with the loss of the strong pain inhibition effect mediated by the *Grp* FFL and thus may be much harder to detect with animal behavioral tests. In a previous study, Mishra and Hoon (2013) ablated 70% of NPR1<sup>+</sup> neurons, which were reported to be a subset of *Grp*<sup>+</sup> neurons, with BNP-conjugated saporin and found a significant change in histamine responses. We believe the partial loss of *Grp*<sup>+</sup> neurons might not be sufficient to generate significant changes in pain responses; however, a trend of increase in pain responses from hot plate test was observed after the ablation of NPR1<sup>+</sup> neurons.

The *Grp*<sup>+</sup> neurons represent a subset of second-order neurons that mediate pain and itch sensations in the spinal cord. Painful stimuli from the periphery can elicit both pain and itch responses via the *Grp*<sup>+</sup> neurons. The itch responses are likely blocked by feedforward inhibition from parallel pain pathways, as noted by the selectivity theory. Similarly, itchy stimuli from the periphery can also trigger both itch and pain responses via the *Grp*<sup>+</sup> neurons. We think this pain responses might be weak, as *Grp*<sup>+</sup> neurons were only weakly activated by itchy stimuli. Indeed, in human psychophysical studies, most itchy substances induce itch sensation accompanied by weaker pain sensations such as pricking and burning, while painful substances induce nociceptive but not itch sensations (LaMotte et al., 2014; Liu et al., 2012; Sikand et al., 2009, 2011a). Even if we cannot rule out the possibility that mechanical or other forms of itch can bypass or block the weak pain responses and result in pure itch sensation, the leaky gate model can explain the nociceptive sensations generated by itchy chemicals in human psychophysics studies.

(F) Pain responses from capsaicin cheek injections (1 mg/mL or 33 nmol, n = 8; 0.5 mg/mL or 16.7 nmol, n = 7 versus 6), capsaicin intraplantar injections (0.1 mg/mL or 3.3 nmol, n = 6; 0.05 mg/mL or 1.67 nmol, n = 6), and immersion assay (50°C, n = 7 versus 6; 52°C, n = 7 versus 6) in *Grp*<sup>Cre</sup>; *ROSA26*<sup>LSL-DTR; LSL-tdTomato</sup> (red) and *ROSA26*<sup>LSL-DTR; LSL-tdTomato</sup> control mice (blue).

(G and H) Pain responses from (G) hot plate test (52°C, n = 10; 55°C, n = 7 versus 6) and Hargreaves test (n = 8 versus 7) as well as (H) Von Frey test responses (n = 11) in *Grp*<sup>Cre</sup>; *ROSA26*<sup>LSL-DTR; LSL-tdTomato</sup> (red) and *ROSA26*<sup>LSL-DTR; LSL-tdTomato</sup> control mice (blue). Yellow shaded regions represent responses with strong stimuli. Data are represented as mean  $\pm$  SEM. \*, p < 0.05; \*\*, p < 0.01; \*\*\*, p < 0.001; extended Welch's t test was used for response ratio comparison between different temperatures in hot plate and tail immersion test, and two-tailed unpaired Student's t test was used for the rest. *Grp*/DTR/tdt is short for *Grp*<sup>Cre</sup>; *ROSA26*<sup>LSL-DTR; LSL-tdTomato</sup>, DTR/tdt is short for *ROSA26*<sup>LSL-DTR; LSL-tdTomato</sup>, CQ is short for chloroquine, and 5-HT is short for serotonin.

In summary, *Grp*<sup>+</sup> neurons positively code for itch while negatively regulating pain transmission with a “leaky gate.” This study, to our knowledge, experimentally demonstrates intensity-dependent coding of pain in the spinal cord for the first time. Our leaky gate model builds on current theories of pain and itch coding and further refines them. It better explains observations in human psychophysical studies and serves as an example of non-monotonic coding and crosstalk of sensory information in the spinal cord. Further studies of the *Grp*<sup>+</sup>-related circuits in chronic pain and itch conditions might uncover relevant changes contributing to these pathological conditions.

## STAR★METHODS

Detailed methods are provided in the online version of this paper and include the following:

- **KEY RESOURCES TABLE**
- **CONTACT FOR REAGENT AND RESOURCE SHARING**
- **EXPERIMENTAL MODEL AND SUBJECT DETAILS**
  - Mouse Lines
- **METHOD DETAILS**
  - Immunofluorescence
  - Electrophysiological Recordings
  - Biocytin Labeling
  - Rabies Viral Tracing
  - ELISA
  - Behavioral Testing
- **QUANTIFICATION AND STATISTICAL ANALYSIS**

## SUPPLEMENTAL INFORMATION

Supplemental Information includes six figures and can be found with this article online at <http://dx.doi.org/10.1016/j.neuron.2017.01.012>.

## AUTHOR CONTRIBUTIONS

S.S. and X.D. initiated the project. S.S. carried out the genetic manipulations, immunostainings, and most of the behavioral experiments. C.G. and Q.L. contributed to optogenetics experiments. Q.X. and Y.G. performed electrophysiological recordings. Q.X. and S.S. performed virus-tracing experiments. S.S. and X.D. wrote the manuscript.

## ACKNOWLEDGMENTS

We thank Dr. Fan Wang at Duke University for deficient rabies virus. We thank C. Hawkins and the staff of the Transgenic Mouse Core at Johns Hopkins University for assistance with transgenic mouse lines. We thank Dr. Hongzhen Hu at Washington University for allowing us to use his optogenetics apparatus. We also thank Dr. Pamela Colleen Lavinka and Dr. Dustin Green at Johns Hopkins University for manuscript editing and Dr. Zhixiang Lin at Stanford University for help with statistics. The work was supported by grants from the National Institutes of Health to X.D. (R01DE022750 and R01NS054791). X.D. is an Investigator of the Howard Hughes Medical Institute.

Received: June 28, 2016

Revised: December 6, 2016

Accepted: January 13, 2017

Published: February 22, 2017

## REFERENCES

- Akiyama, T., Carstens, M.I., and Carstens, E. (2009a). Excitation of mouse superficial dorsal horn neurons by histamine and/or PAR-2 agonist: potential role in itch. *J. Neurophysiol.* *102*, 2176–2183.
- Akiyama, T., Merrill, A.W., Carstens, M.I., and Carstens, E. (2009b). Activation of superficial dorsal horn neurons in the mouse by a PAR-2 agonist and 5-HT: potential role in itch. *J. Neurosci.* *29*, 6691–6699.
- Alon, U. (2007). Network motifs: theory and experimental approaches. *Nat. Rev. Genet.* *8*, 450–461.
- Bell, A.M., Gutierrez-Mecinas, M., Polgár, E., and Todd, A.J. (2016). Spinal neurons that contain gastrin-releasing peptide seldom express Fos or phosphorylate extracellular signal-regulated kinases in response to intradermal chloroquine. *Mol. Pain* *12*, 1744806916649602, <http://dx.doi.org/10.1177/1744806916649602>.
- Bourane, S., Duan, B., Koch, S.C., Dalet, A., Britz, O., Garcia-Campmany, L., Kim, E., Cheng, L., Ghosh, A., Ma, Q., and Goulding, M. (2015). Gate control of mechanical itch by a subpopulation of spinal cord interneurons. *Science* *350*, 550–554.
- Braz, J., Solorzano, C., Wang, X., and Basbaum, A.I. (2014). Transmitting pain and itch messages: a contemporary view of the spinal cord circuits that generate gate control. *Neuron* *82*, 522–536.
- Cesselin, F., Bourgoin, S., Artaud, F., and Hamon, M. (1984). Basic and regulatory mechanisms of in vitro release of Met-enkephalin from the dorsal zone of the rat spinal cord. *J. Neurochem.* *43*, 763–774.
- Davidson, S., Zhang, X., Yoon, C.H., Khasabov, S.G., Simone, D.A., and Giesler, G.J., Jr. (2007). The itch-producing agents histamine and cowhage activate separate populations of primate spinothalamic tract neurons. *J. Neurosci.* *27*, 10007–10014.
- Davidson, S., Zhang, X., Khasabov, S.G., Simone, D.A., and Giesler, G.J., Jr. (2009). Relief of itch by scratching: state-dependent inhibition of primate spinothalamic tract neurons. *Nat. Neurosci.* *12*, 544–546.
- Davidson, S., Zhang, X., Khasabov, S.G., Moser, H.R., Honda, C.N., Simone, D.A., and Giesler, G.J., Jr. (2012). Prurceptive spinothalamic tract neurons: physiological properties and projection targets in the primate. *J. Neurophysiol.* *108*, 1711–1723.
- Duan, B., Cheng, L., Bourane, S., Britz, O., Padilla, C., Garcia-Campmany, L., Krashes, M., Knowlton, W., Velasquez, T., Ren, X., et al. (2014). Identification of spinal circuits transmitting and gating mechanical pain. *Cell* *159*, 1417–1432.
- Fleming, M.S., Ramos, D., Han, S.B., Zhao, J., Son, Y.-J., and Luo, W. (2012). The majority of dorsal spinal cord gastrin releasing peptide is synthesized locally whereas neuromedin B is highly expressed in pain- and itch-sensing somatosensory neurons. *Mol. Pain* *8*, 52.
- Fukushima, T., Tsuda, M., Kofuji, T., and Hori, Y. (2011). Physiological properties of enkephalin-containing neurons in the spinal dorsal horn visualized by expression of green fluorescent protein in BAC transgenic mice. *BMC Neurosci.* *12*, 36.
- Gong, S., Zheng, C., Doughty, M.L., Losos, K., Didkovsky, N., Schambra, U.B., Nowak, N.J., Joyner, A., Leblanc, G., Hatten, M.E., and Heintz, N. (2003). A gene expression atlas of the central nervous system based on bacterial artificial chromosomes. *Nature* *425*, 917–925.
- Grudt, T.J., and Perl, E.R. (2002). Correlations between neuronal morphology and electrophysiological features in the rodent superficial dorsal horn. *J. Physiol.* *540*, 189–207.
- Han, S.-K., Mancino, V., and Simon, M.I. (2006). Phospholipase Cbeta 3 mediates the scratching response activated by the histamine H1 receptor on C-fiber nociceptive neurons. *Neuron* *52*, 691–703.
- Han, L., Ma, C., Liu, Q., Weng, H.-J., Cui, Y., Tang, Z., Kim, Y., Nie, H., Qu, L., Patel, K.N., et al. (2013). A subpopulation of nociceptors specifically linked to itch. *Nat. Neurosci.* *16*, 174–182.
- Handwerker, H.O. (1992). Pain and allodynia, itch and allodynia: An alternative hypothesis. *J. Pain* *1*, 135–138.

- Handwerker, H.O., Forster, C., and Kirchhoff, C. (1991). Discharge patterns of human C-fibers induced by itching and burning stimuli. *J. Neurophysiol.* *66*, 307–315.
- Hunnskaar, S., Fasmer, O.B., and Hole, K. (1985). Acetylsalicylic acid, paracetamol and morphine inhibit behavioral responses to intrathecally administered substance P or capsaicin. *Life Sci.* *37*, 1835–1841.
- Hunnskaar, S., Post, C., Fasmer, O.B., and Arwestrom, E. (1986). Intrathecal injection of capsaicin can be used as a behavioural nociceptive test in mice. *Neuropharmacology* *25*, 1149–1153.
- Kardon, A.P., Polgár, E., Hachisuka, J., Snyder, L.M., Cameron, D., Savage, S., Cai, X., Karnup, S., Fan, C.R., Hemenway, G.M., et al. (2014). Dynorphin acts as a neuromodulator to inhibit itch in the dorsal horn of the spinal cord. *Neuron* *82*, 573–586.
- LaMotte, R.H., Shimada, S.G., and Sikand, P. (2011). Mouse models of acute, chemical itch and pain in humans. *Exp. Dermatol.* *20*, 778–782.
- LaMotte, R.H., Dong, X., and Ringkamp, M. (2014). Sensory neurons and circuits mediating itch. *Nat. Rev. Neurosci.* *15*, 19–31.
- Lee, H., and Ko, M.-C. (2015). Distinct functions of opioid-related peptides and gastrin-releasing peptide in regulating itch and pain in the spinal cord of primates. *Sci. Rep.* *5*, 11676.
- Lewis, T., Grant, R.T., and Marvin, H.M. (1927). Vascular reactions of the skin to injury, part X: the intervention of a chemical stimulus illustrated especially by flare. The response to faradism. *Heart* *14*, 139–160.
- Liu, Q., Tang, Z., Surdenikova, L., Kim, S., Patel, K.N., Kim, A., Ru, F., Guan, Y., Weng, H.-J., Geng, Y., et al. (2009). Sensory neuron-specific GPCR Mrgpr8 are itch receptors mediating chloroquine-induced pruritus. *Cell* *139*, 1353–1365.
- Liu, Q., Weng, H.-J., Patel, K.N., Tang, Z., Bai, H., Steinhoff, M., and Dong, X. (2011). The distinct roles of two GPCRs, MrgprC11 and PAR2, in itch and hyperalgesia. *Sci. Signal.* *4*, ra45.
- Liu, Q., Sikand, P., Ma, C., Tang, Z., Han, L., Li, Z., Sun, S., LaMotte, R.H., and Dong, X. (2012). Mechanisms of itch evoked by  $\beta$ -alanine. *J. Neurosci.* *32*, 14532–14537.
- McMahon, S.B., and Koltzenburg, M. (1992). Itching for an explanation. *Trends Neurosci.* *15*, 497–501.
- Melzack, R., and Wall, P.D. (1965). Pain mechanisms: a new theory. *Science* *150*, 971–979.
- Milo, R., Shen-Orr, S., Itzkovitz, S., Kashtan, N., Chklovskii, D., and Alon, U. (2002). Network motifs: simple building blocks of complex networks. *Science* *298*, 824–827.
- Mishra, S.K., and Hoon, M.A. (2013). The cells and circuitry for itch responses in mice. *Science* *340*, 968–971.
- Nakatsuka, T., Ataka, T., Kumamoto, E., Tamaki, T., and Yoshimura, M. (2000). Alteration in synaptic inputs through C-afferent fibers to substantia gelatinosa neurons of the rat spinal dorsal horn during postnatal development. *Neuroscience* *99*, 549–556.
- Neuman, B., Wiedermann, C.J., Fischer-Colbrie, R., Schober, M., Sperk, G., and Winkler, H. (1984). Biochemical and functional properties of large and small dense-core vesicles in sympathetic nerves of rat and ox vas deferens. *Neuroscience* *13*, 921–931.
- Norsrill, U., Finger, S., and Lajonchere, C. (1999). Cutaneous sensory spots and the “law of specific nerve energies”: history and development of ideas. *Brain Res. Bull.* *48*, 457–465.
- Ochoa, J., and Torebjörk, E. (1989). Sensations evoked by intraneural microstimulation of C nociceptor fibres in human skin nerves. *J. Physiol.* *415*, 583–599.
- Schmelz, M., Schmidt, R., Bickel, A., Handwerker, H.O., and Torebjörk, H.E. (1997). Specific C-receptors for itch in human skin. *J. Neurosci.* *17*, 8003–8008.
- Schmelz, M., Schmidt, R., Weidner, C., Hilliges, M., Torebjörk, H.E., and Handwerker, H.O. (2003). Chemical response pattern of different classes of C-nociceptors to pruritogens and algogens. *J. Neurophysiol.* *89*, 2441–2448.
- Sikand, P., Shimada, S.G., Green, B.G., and LaMotte, R.H. (2009). Similar itch and nociceptive sensations evoked by punctate cutaneous application of capsaicin, histamine and cowhage. *Pain* *144*, 66–75.
- Sikand, P., Dong, X., and LaMotte, R.H. (2011a). BAM8-22 peptide produces itch and nociceptive sensations in humans independent of histamine release. *J. Neurosci.* *31*, 7563–7567.
- Sikand, P., Shimada, S.G., Green, B.G., and LaMotte, R.H. (2011b). Sensory responses to injection and punctate application of capsaicin and histamine to the skin. *Pain* *152*, 2485–2494.
- Solorzano, C., Villafuerte, D., Meda, K., Cevikbas, F., Bráz, J., Sharif-Naeini, R., Juarez-Salinas, D., Llewellyn-Smith, I.J., Guan, Z., and Basbaum, A.I. (2015). Primary afferent and spinal cord expression of gastrin-releasing peptide: message, protein, and antibody concerns. *J. Neurosci.* *35*, 648–657.
- Spike, R.C., Puskár, Z., Andrew, D., and Todd, A.J. (2003). A quantitative and morphological study of projection neurons in lamina I of the rat lumbar spinal cord. *Eur. J. Neurosci.* *18*, 2433–2448.
- Sun, Y.-G., and Chen, Z.-F. (2007). A gastrin-releasing peptide receptor mediates the itch sensation in the spinal cord. *Nature* *448*, 700–703.
- Sun, Y.-G., Zhao, Z.-Q., Meng, X.-L., Yin, J., Liu, X.-Y., and Chen, Z.-F. (2009). Cellular basis of itch sensation. *Science* *325*, 1531–1534.
- Todd, A.J. (2010). Neuronal circuitry for pain processing in the dorsal horn. *Nat. Rev. Neurosci.* *11*, 823–836.
- Todd, A.J., Spike, R.C., Russell, G., and Johnston, H.M. (1992). Immunohistochemical evidence that Met-enkephalin and GABA coexist in some neurones in rat dorsal horn. *Brain Res.* *584*, 149–156.
- Tuckett, R.P. (1982). Itch evoked by electrical stimulation of the skin. *J. Invest. Dermatol.* *79*, 368–373.
- Von Frey, M. (1922). Zur physiologie der juckempfindung. *Arch. Neurol. Physiol* *7*, 142.
- Wall, P.D. (1978). The gate control theory of pain mechanisms. A re-examination and re-statement. *Brain* *101*, 1–18.
- Wickersham, I.R., Lyon, D.C., Barnard, R.J.O., Mori, T., Finke, S., Conzelmann, K.-K., Young, J.A.T., and Callaway, E.M. (2007). Monosynaptic restriction of transsynaptic tracing from single, genetically targeted neurons. *Neuron* *53*, 639–647.
- Yaksh, T.L., Farb, D.H., Leeman, S.E., and Jessell, T.M. (1979). Intrathecal capsaicin depletes substance P in the rat spinal cord and produces prolonged thermal analgesia. *Science* *206*, 481–483.

## STAR★METHODS

## KEY RESOURCES TABLE

REAGENT or RESOURCE	SOURCE	IDENTIFIER
<b>Antibodies</b>		
rabbit anti-CGRP	Peninsula	Cat# T-4239; RRID: AB_518150
rabbit anti-NF200	Chemicon	Cat# AB1982; RRID: AB_2313731
rabbit anti-PKC $\gamma$	Santa Cruz Biotechnology	Cat# sc-211; RRID: AB_632234
rabbit anti-GFP	Molecular Probes	Cat# A-11122; RRID: AB_221569
mouse anti-Neuronal nuclei	Chemicon	Cat# MAB377; RRID: AB_2298767
mouse anti-PSD95	NeuroMab	Cat# K28/43; RRID: AB_2315221
rabbit anti-PSD95	Millipore	Cat# 04-1066; RRID: AB_1977415
guinea pig anti-TrpV1	Millipore	Cat# AB5566; RRID: AB_91901
rabbit anti-MrgprC11	(Han et al., 2013)	N/A
mouse anti-GAD1	Millipore	Cat# MAB 5406; RRID: AB_2278725
mouse anti-Enkephalin	Millipore	Cat# NOC1; RRID: AB_2268028
goat anti-rabbit Alexa 488 conjugated	Thermo Fisher	Cat# A11008; RRID: AB_143165
goat anti-rabbit Alexa 568 conjugated	Thermo Fisher	Cat# A11011; RRID: AB_143157
goat anti-rabbit Alexa 647 conjugated	Thermo Fisher	Cat# A21245; RRID: AB_2535813
goat anti-mouse Alexa 488 conjugated	Thermo Fisher	Cat# A11001; RRID: AB_2534069
goat anti-mouse Alexa 568 conjugated	Thermo Fisher	Cat# A11004; RRID: AB_141371
goat anti-mouse Alexa 647 conjugated	Thermo Fisher	Cat# A21236; RRID: AB_141725
goat anti-guinea pig Alexa 568 conjugated	Thermo Fisher	Cat# A11075; RRID: AB_141954
isolectin GS-IB4 Alexa 488 conjugated	Thermo Fisher	Cat# I21411; RRID: AB_2314662
isolectin GS-IB4 Alexa 568 conjugated	Thermo Fisher	Cat# I21412
<b>Chemicals, Peptides, and Recombinant Proteins</b>		
Alexa 488 conjugated streptavidin	Life technologies	Cat# S11223
diphtheria toxin	Sigma	Cat# D0564
Deamino-Phe <sup>19</sup> , D-Ala <sup>24</sup> , D-Pro <sup>26</sup> -psi(CH <sub>2</sub> NH)Phe <sup>27</sup> -GRP (19-27)	Bachem	Cat# H-2756
naloxone	Sigma	Cat# N7758
naltrindole	Sigma	Cat# N115
CTAP	Sigma	Cat# C6352
CTOP	Sigma	Cat# P5296
CycloSOM	Tocris	Cat# 3493
bicuculline	Sigma	Cat# 14343
GRP	Sigma	Cat# G8022
BNP	Sigma	Cat# B9901
Alexa 568 dye	life technologies	Cat# A20003
<b>Critical Commercial Assays</b>		
Enkephalin ELISA kit	Phoenix Pharmaceuticals	Cat# FEK02421
<b>Experimental Models: Organisms/Strains</b>		
Mouse: <i>Grp</i> <sup>Cre</sup>	MMRRC	MMRRC_037585-UCD
Mouse: <i>Grp</i> <sup>EGFP</sup>	MMRRC	MMRRC_010444-UCD
Mouse: <i>MrgprA3</i> <sup>Cre</sup>	(Han et al., 2013)	N/A
Mouse: <i>ROSA26</i> <sup>LSL-tdTomato</sup>	Jackson lab	Jax: 007908
Mouse: <i>ROSA26</i> <sup>LSL-ChR2</sup>	Jackson lab	Jax: 012569
Mouse: <i>ROSA26</i> <sup>LSL-DTR</sup>	Jackson lab	Jax: 007900

(Continued on next page)

**Continued**

REAGENT or RESOURCE	SOURCE	IDENTIFIER
Mouse: <i>ROSA26<sup>LSL-TrpV1</sup></i>	Jackson lab	Jax: 008513
Mouse: <i>vGlut2<sup>Cre</sup></i>	Jackson lab	Jax: 016963
Mouse: <i>GAD1<sup>EGFP</sup></i>	Jackson lab	Jax: 007677
Mouse: <i>TrpV1<sup>-/-</sup></i>	Jackson lab	Jax: 003770
Software and Algorithms		
R	r-project.org	R 3.3.2
pClamp 10	Molecular Devices	N/A
Other		
AAV8-LSL-TVA-EGFP-B19G	UNC vector core	Addgene 52473
AAV2/1-FLEX-tdTomato	Upenn vector core	Cat# V1677
EnvA pseudotyped rabies glycoprotein deficient GFP rabies virus	Dr. Fan Wang's lab	N/A
isoflurane	Abbott Laboratories	CAS# 26675-46-7
Fully automated vibrating blade microtome	Leica Biosystems	VT1200
Micropipette Puller	Sutter	P1000
Pulse Stimulator	AMPI	Master-9
Iso-Flex Stimulus Isolator	AMPI	N/A
LED illumination system	Brainvision	LEX2-B
Rotarod	Columbus Instruments	Rotamex 5

**CONTACT FOR REAGENT AND RESOURCE SHARING**

Further information and requests for resources and reagents should be directed to and will be fulfilled by the Lead Contact, Xinzhong Dong ([xdong2@jhmi.edu](mailto:xdong2@jhmi.edu)).

**EXPERIMENTAL MODEL AND SUBJECT DETAILS****Mouse Lines**

*Grp<sup>Cre</sup>* and *Grp<sup>EGFP</sup>* mouse lines were acquired from MMRRC. *MrgprA3<sup>Cre</sup>* mouse line was previously generated by our group. *ROSA26<sup>LSL-tdTomato</sup>*, *ROSA26<sup>LSL-ChR2</sup>*, *ROSA26<sup>LSL-DTR</sup>*, *ROSA26<sup>LSL-TrpV1</sup>*, *vGlut2<sup>Cre</sup>*, *GAD1<sup>EGFP</sup>* and *TrpV1<sup>-/-</sup>* mouse lines were acquired from the Jackson laboratory. We used *Grp<sup>Cre</sup>*, *Grp<sup>EGFP</sup>*, and *MrgprA3<sup>Cre</sup>* as hemizygotes or heterozygotes for all the experiments. All experiments were performed using protocols approved by the Animal Care and Use Committee of Johns Hopkins University School of Medicine.

All behavioral tests were performed with an experimenter blind to genotype. The mice were 2–4-month-old males that had been backcrossed to C57BL/6 mice for at least six generations. The day before the behavioral tests, all mice were acclimated for at least 30 min to their testing environment. We housed 4–5 mice in each cage in the vivarium with 12h light/dark cycle and all the behavioral tests were performed in the morning.

**METHOD DETAILS****Immunofluorescence**

2–4 month old mice were anesthetized with pentobarbital and perfused with 20 mL 0.1 M PBS (pH 7.4, 4°C) followed with 25 mL of fixative (4% formaldehyde (vol/vol) and 14% sat. picric acid (vol/vol) in PBS, 4°C). Spinal cord and DRG were dissected from the perfused mice. DRG was postfixed in fixative at 4°C for 30 min, and spinal cord were fixed for 1 hr. Tissues were cryoprotected in 30% sucrose (wt/vol) for more than 12 hr and were sectioned with a cryostat. The sections on slides were dried at 37°C for 40 min, and fixed with 4% paraformaldehyde at room temperature for 10 min. The slides were preincubated in blocking solution (10% normal goat serum (vol/vol), 0.2% Triton X-100 (vol/vol) in PBS, pH 7.4) for 1 or 2 hr at room temperature, then incubated overnight at 4°C with primary antibodies. Secondary antibody incubation was performed at room temperature for 2 hr.

For primary antibodies, we used rabbit  $\alpha$ -CGRP (T-4239, Peninsula, 1:1,000), rabbit  $\alpha$ -NF200 (AB1982, Chemicon, 1:1,000), rabbit  $\alpha$ -PKC $\gamma$  (sc-211, Santa Cruz Biotechnology, 1:1,000), rabbit  $\alpha$ -GFP (A-11122, Molecular Probes, 1:1,000), mouse  $\alpha$ -Neuronal nuclei (MAB377, Chemicon, 1:200), mouse  $\alpha$ -PSD95 (K28/43, NeuroMab, 1:500), rabbit  $\alpha$ -PSD95 (EP1183Y, Millipore, 1:500), guinea pig  $\alpha$ -TrpV1 (AB5566, Millipore, 1:200), rabbit  $\alpha$ -MrgprC11 (made by our lab, 1:200), mouse  $\alpha$ -GAD1 (MAB 5406, Millipore, 1:2000)

and mouse  $\alpha$ -Enkephalin (NOC1, Millipore, 1:100). For secondary antibodies, we used goat  $\alpha$ -rabbit (A11008, Alexa 488 conjugated; A11011, Alexa 568 conjugated; A21245, Alexa 647 conjugated, Thermo Fisher), goat  $\alpha$ -mouse (A11001, Alexa 488 conjugated; A11004, Alexa 568 conjugated; A21236, Alexa 647 conjugated, Thermo Fisher) and goat  $\alpha$ -guinea pig (A11075, Alexa 568 conjugated). All secondary antibodies were diluted 1:500 in blocking solution. To detect IB4 binding, sections were incubated with Griffonia simplicifolia isolectin GS-IB4 (1:500; I21411, Alexa 488 conjugated; I21412, Alexa 568 conjugated, Thermo Fisher).

### Electrophysiological Recordings

To prepare spinal cord slices, 4 to 6 week-old mice were deeply anesthetized with 2% isoflurane (Abbott Laboratories, North Chicago, IL, USA). Spinal cord with dorsal root or DRG was rapidly removed and placed in ice-cold, low-sodium Krebs solution that contained: 95mM NaCl, 2.5mM KCl, 26mM NaHCO<sub>3</sub>, 1.25mM NaH<sub>2</sub>PO<sub>4</sub>-H<sub>2</sub>O, 6mM MgCl<sub>2</sub>, 1.5mM CaCl<sub>2</sub>, 25mM glucose, 50mM sucrose, 1mM kynurenic acid bubbled with 95% O<sub>2</sub>/5% CO<sub>2</sub>. Sagittal spinal cord slices (400  $\mu$ m) with dorsal roots or DRG attached were cut by a Vibratome (VT1200, Leica Biosystems, Buffalo Grove, IL, USA) and transferred to low-sodium Krebs solution without kynurenic acid for recovery at 34°C for 45 min and then at room temperature for an additional 1 hr before being used for recordings.

For electrophysiology recording, slices were stabilized with a nylon harp and submerged in a low-volume recording chamber (SD Instruments, San Diego, CA, USA), which was perfused with Krebs solution (125mM NaCl, 2.5mM KCl, 26mM NaHCO<sub>3</sub>, 1.25mM NaH<sub>2</sub>PO<sub>4</sub>-H<sub>2</sub>O, 1mM MgCl<sub>2</sub>, 2mM CaCl<sub>2</sub>, 25mM glucose) at a rate of 5ml/min bubbled with 95% O<sub>2</sub>/5% CO<sub>2</sub>. Whole-cell patch-clamp recording of Grp<sup>+</sup> neuron was carried out under oblique illumination with an Olympus fixed-stage microscope system (BX51, Melville, NY, USA). Using a puller (P1000, Sutter, Novato, CA, USA), we fabricated thin-walled glass pipettes (World Precision Instruments, Sarasota, FL, USA) that had a resistance of 3-6 M $\Omega$  and were filled with internal solution (120mM K-gluconate, 20mM KCl, 2mM MgCl<sub>2</sub>, 0.5mM EGTA, 2mM Na<sub>2</sub>-ATP, 0.5mM Na<sub>2</sub>-GTP, and 20mM HEPES). The cells were voltage clamped at -70 mV. Membrane current signals were sampled at 10kHz and low-pass filtered at 2 kHz. We monitored R series and R input and discarded cells if either of these values changed by more than 20%.

DRGs were collected from mice, which were deeply anesthetized with 2% isoflurane (Abbott Laboratories, North Chicago, IL, USA) and put in cold DH10 medium (DMEM/F-12 with 10% fetal bovine serum and 1% penicillin/streptomycin, GIBCO) and treated with enzyme solution (5mg/ml dispase and 1mg/ml collagenase Type I in HBSS without Ca<sup>2+</sup> and Mg<sup>2+</sup>, GIBCO) at 37°C. After trituration and centrifugation, cells were resuspended in DH10 with nerve growth factor (50 ng/ml, Upstate) and glial cell line-derived neurotrophic factor (25 ng/ml, R&D Systems), plated on glass coverslips coated with poly-D-lysine (100  $\mu$ g/ml, Biomedical Technologies) and laminin (10  $\mu$ g/ml, Invitrogen), cultured at 37°C, and used after 20–40 hr. Whole-cell recording of MrgprA3 positive DRG neurons were performed with Axon 700B amplifier and pClamp 10 software (Molecular Devices, Sunnyvale, CA). The thin-walled glass pipettes were pulled by a puller (P1000, Sutter, Novato, CA, USA) with the resistance of 2-4 M $\Omega$ .

Dorsal-root stimulation was applied by a suction electrode at 500  $\mu$ A, sufficient to activate C-fibers, using a Master-9 Pulse Stimulator and Iso-Flex Stimulus Isolator (AMPI, Jerusalem, Israel). For light stimulation mediated by channelrhodopsin, the LED blue light (465 nm, 300 mW/cm<sup>2</sup>) was elicited by a high power LED illumination system (LEX2-B, Brainvision) through the Olympus fixed-stage microscope system (BX51, Melville, NY, USA). The LED illumination system was connected to an A/D converter (Digidata 1440, Axon CNS, Molecular Devices), and controlled by the pClamp10 software (Axon CNS). For DRG attached spinal cord slice Grp neurons recording, drugs were directly puffed on the DRG tissue using the DVD-8VC superfusion application system (ALA Scientific Instruments, Farmingdale, NY, USA). To differentiate monosynaptic and polysynaptic connections, 20 C-fiber-strength electrical stimulation or light stimulation at 1 Hz were delivered, neurons with no failure in EPSCs were monosynaptically connected according to established criteria (Nakatsuka et al., 2000).

Calcium imaging of enkephalin-expression neurons was performed with a 700 Zeiss confocal microscope. *Penk<sup>Cre</sup>; Rosa26<sup>LSL-GCaMP6</sup>; Grp<sup>EGFP</sup>* spinal slices were cut as described above. The *Grp<sup>EGFP</sup>* neurons were patched and depolarized by 1 Hz 50pA current injection. Green fluorescence of patch neurons was monitored to exclude recording of active *Penk<sup>+</sup>* neurons. Patched *Grp<sup>EGFP</sup>* neurons were labeled by Red fluorescent dye (Alex Fluor 568, life technologies). Images were acquired at 2.6Hz in frame-scan mode with a 256  $\times$  256 pixel region of interest.

### Biocytin Labeling

After 20 min in the whole-cell patch-clamp configuration, the biocytin-filled (0.5%) electrodes were withdrawn from the targeted neuron, and the slices were immersed in 4% paraformaldehyde for 15 min. Spinal slices were then washed with PBS (3 X 20 min) and incubated with Alexa 488 conjugated streptavidin (1:200, Life technologies) at 4°C overnight. After washing with PBS (3 X 20 min), the fluorescent signals of the spinal cord sections were collected as z series images using a confocal microscope.

### Rabies Viral Tracing

Mice were anesthetized by isoflurane and a laminectomy was performed at the T13-L1 level. A fine glass capillary was inserted into dorsal spinal cord. AAV helper virus, AAV8-LSL-TVA-EGFP-B19G (UNC vector core), was first injected (500nl, 50nl/min). AAV1-LSL-tdTomato virus (Upenn vector core) was similarly injected to visualize *Grp<sup>+</sup>* neurons. EnvA pseudotyped rabies glycoprotein deficient GFP rabies virus (Courtesy of Dr. Fan Wang's group, Duke University) was injected in the same spot 3 weeks later. Animals were perfused 7 days after rabies virus injection and processed for immunostaining.

## ELISA

*Grp<sup>Cre</sup>; ROSA26<sup>LSL-TrpV1</sup>; TrpV1<sup>-/-</sup>* mice and *ROSA26<sup>LSL-TrpV1</sup>; TrpV1<sup>-/-</sup>* littermate controls were deeply anesthetized with isoflurane, decapitated and the lumbar spinal cord was quickly removed to ice-cold, low-sodium Krebs solution that contained: 95 mM NaCl, 2.5 mM KCl, 26 mM NaHCO<sub>3</sub>, 1.25 mM NaH<sub>2</sub>PO<sub>4</sub>-H<sub>2</sub>O, 6 mM MgCl<sub>2</sub>, 1.5 mM CaCl<sub>2</sub>, 25 mM glucose, 50 mM sucrose, 1 mM kynurenic acid bubbled with 95% O<sub>2</sub>/5% CO<sub>2</sub>. Spinal cords were cut into three sagittal sections and then recovered in oxygenated ACSF for about 1 hr at 37°C. Three sections were subsequently incubated with 200 μL oxygenated Krebs solution (125 mM NaCl, 2.5 mM KCl, 26 mM NaHCO<sub>3</sub>, 1.25 mM NaH<sub>2</sub>PO<sub>4</sub>-H<sub>2</sub>O, 1 mM MgCl<sub>2</sub>, 2 mM CaCl<sub>2</sub>, 25 mM glucose) with capsaicin (2 mg/mL, 5 μg/mL and 0 μg/mL, respectively) and proteinase inhibitor mix (1 μM phosphoramidon, 1 μM captopril, and 0.1% BSA) for 15 min at 37°C. 100 μL of ACSF from each sample was then used for the detection of Enkephalin release. ELISA detections of enkephalin were performed following manufacturer's protocol (FEK02421, Phoenix Pharmaceuticals). Results were normalized to the weight of the tissue. At least six mice were used for each condition.

## Behavioral Testing

For ablation experiments, we injected 8-week-old *Grp<sup>Cre</sup>; ROSA26<sup>LSL-DTR;LSL-tdTomato</sup>* mice and *ROSA26<sup>LSL-DTR;LSL-tdTomato</sup>* littermates with diphtheria toxin (intraperitoneal, 35 μg per kg of body weight, Sigma) twice, separated by 72 hr. Behavioral experiments were performed 4 weeks after the first toxin injection.

For back injections, pruritic compounds dissolved in saline were subcutaneously injected into the nape of the neck (50 μl) with insulin syringes (26 Gauge). GRPR antagonist (Deamino-Phe<sup>19</sup>,D-Ala<sup>24</sup>,D-Pro<sup>26</sup>-psi(CH<sub>2</sub>NH)Phe<sup>27</sup>)-GRP (19-27), 200 μM or 2 nmol/site or saline (50 μl) were injected 10 min before pruritogen injection when indicated. Behavioral responses were video recorded for 30 min. The video recording was subsequently played back in slow motion and the number of bouts of scratching with the hindpaw and directed toward the injection site, were counted.

For the hot plate test, a clear plexiglass cylinder was placed on the plate and the mice were placed inside the cylinder. The onset of brisk hindpaw lifts and/or flicking/licking of the hindpaw was assessed at different temperatures.

For the tail immersion test, mice were gently restrained in a 50 mL conical tube into which the mice voluntarily entered. The protruding one-third of the tail was then dipped into a water bath of varying temperatures. The latency to respond to the heat stimulus with vigorous flexion of the tail was measured.

For the Hargreaves test, mice were placed under a transparent plastic box (4.5 × 5 × 10 cm) on a glass floor. The infrared source was placed under the glass floor and the infrared light was delivered to the hindpaw. The latency for the animal to withdraw its hindpaw was measured.

For the Von Frey filament test, mice were placed under a transparent plastic box (4.5 × 5 × 10 cm) on a metal mesh. Von Frey filaments, each delivering a different bending force, were applied to the hind paw using the up-down method and the threshold force corresponding to 50% withdrawal was determined.

For the chemically induced pain test, 10 μL of capsaicin and 7 μL of capsaicin were injected in cheek and paw respectively and the numbers of front paw wipes or the time of licking/flinching responses were counted in 10 min.

For the rotarod test, each mouse was trained for 5 min at a constant speed of 4 rpm on the rotarod (Rotamex, Columbus Instruments). The first trial started at least 1 hr after training. Every day, each mouse received three trials, separated by 30 min, at speeds accelerating from 4 to 40 rpm (with a 4 rpm increase every 30 s). Each mouse was tested for 3 consecutive days. The trial was finished when the mouse fell off the rotarod. The latency to falling off the rotarod was recorded and used in subsequent analyses.

For specific activation of *Grp<sup>+</sup>* neurons, *Grp<sup>Cre</sup>; ROSA26<sup>LSL-TrpV1</sup>; TrpV1<sup>-/-</sup>* mice were intrathecally injected with different amounts of capsaicin or capsaicin with naloxone (0.1 mg/mL), naltrindole (0.2 mg/mL), CTAP (0.5 mg/mL), CTOP (1 mg/mL), cycloSOM (0.1 mM) and bicuculline (10 μM). Lumbar puncture were made with 30 gauge needles and drugs at 10 μL of volume were delivered. Lower back regions of mice were shaved a day before injections. High definition videos were recorded from the top for 30 min with four mirrors to enable views of all angles. Video recordings were subsequently played back at 1/5 normal speed. The durations of licking directed to lower back region with a characteristic frequency of 5 Hz were quantified in the first 4 min and bouts of scratching were counted in 30 min. *ROSA26<sup>LSL-TrpV1</sup>; TrpV1<sup>-/-</sup>* littermates were used as controls. Wild-type and *TrpV1<sup>-/-</sup>* mice were also intrathecally injected with GRP, BNP and capsaicin. Licking and scratching behaviors quantified as reference.

For light mediated activation of *MrgprA3<sup>+</sup>* neurons, *MrgprA3<sup>Cre</sup>; ROSA26<sup>LSL-ChR2</sup>* mice with shaved nape regions were given 100 ms blue light at 1 Hz or 5 Hz and litter mate *ROSA26<sup>LSL-ChR2</sup>* mice were used as controls. Scratching bouts were counted in 5 min time periods. Sham operations without blue light were used to determine baseline scratch numbers.

## QUANTIFICATION AND STATISTICAL ANALYSIS

Data are presented as mean ± SEM. n represents the number of mice analyzed. The distribution of the variables in each experimental group was assumed normal. Most statistical comparisons were conducted by two-tailed, unpaired Student's t test. Two-way ANOVA followed by post hoc Student-Newmann-Keuls tests were used for comparison between capsaicin and pruritogen-induced responses. Extended Welch's t test was used for the comparison of ratios of ablated responses and control responses, where Student's t tests and ANOVA tests could not apply. Power analysis was used to justify the sample size. No data were excluded.

Differences were considered to be statistically significant for  $p < 0.05$ . Representative data are from experiments that were replicated biologically at least three times with similar results. Statistical analysis done with R.

Extension of Welch's t test:  $\mu_{1h}$ : mean of log value of ablated responses, high dose;  $\mu_{1l}$ : mean of log value of ablated responses, low dose;  $\mu_{2h}$ : mean of log value of control responses, high dose;  $\mu_{2l}$ : mean of log value of control responses, low dose. Null hypothesis  $H_0: (\mu_{1h} - \mu_{2h}) - (\mu_{1l} - \mu_{2l}) = 0$ . Alternative  $H_1: (\mu_{1h} - \mu_{2h}) - (\mu_{1l} - \mu_{2l}) > 0$ . Test statistics:  $t = \frac{(\bar{\mu}_{1h} - \bar{\mu}_{2h}) - (\bar{\mu}_{1l} - \bar{\mu}_{2l})}{s}$ , where  $\bar{\mu}$  denotes the sample means of the subgroup.  $s = \sqrt{(s_{1h}^2/n_{1h}) + (s_{1l}^2/n_{1l}) + (s_{2h}^2/n_{2h}) + (s_{2l}^2/n_{2l})}$ , where  $s^2$  denotes the sample variance and  $n$  is the sample size. Under  $H_0$ , the test statistics follows t-distribution and the degrees of freedom,

$$df = \frac{\left( s_{1h}^2/n_{1h} + s_{2h}^2/n_{2h} + s_{1l}^2/n_{1l} + s_{2l}^2/n_{2l} \right)^2}{\left( s_{1h}^2/n_{1h} \right)^2 / (n_{1h} - 1) + \left( s_{2h}^2/n_{2h} \right)^2 / (n_{2h} - 1) + \left( s_{1l}^2/n_{1l} \right)^2 / (n_{1l} - 1) + \left( s_{2l}^2/n_{2l} \right)^2 / (n_{2l} - 1)}$$

Dose response curve fitting for capsaicin mediated activation:

lch dose responses were fit with Hill equation:

$$y = 7.946 + \frac{154.854}{1 + 10^{(0.495-x) \times 0.5577}}$$

Pain dose responses were fit with polynomial equation:

$$y = 0.469 - 3.882x + 11.38x^2 - 1.904x^3 + 0.08229x^4.$$

**Neuron, Volume 93**

**Supplemental Information**

**Leaky Gate Model: Intensity-Dependent Coding  
of Pain and Itch in the Spinal Cord**

**Shuohao Sun, Qian Xu, Changxiong Guo, Yun Guan, Qin Liu, and Xinzhong Dong**

## Supplemental Figures and Supplemental Video Legends

Figure S1

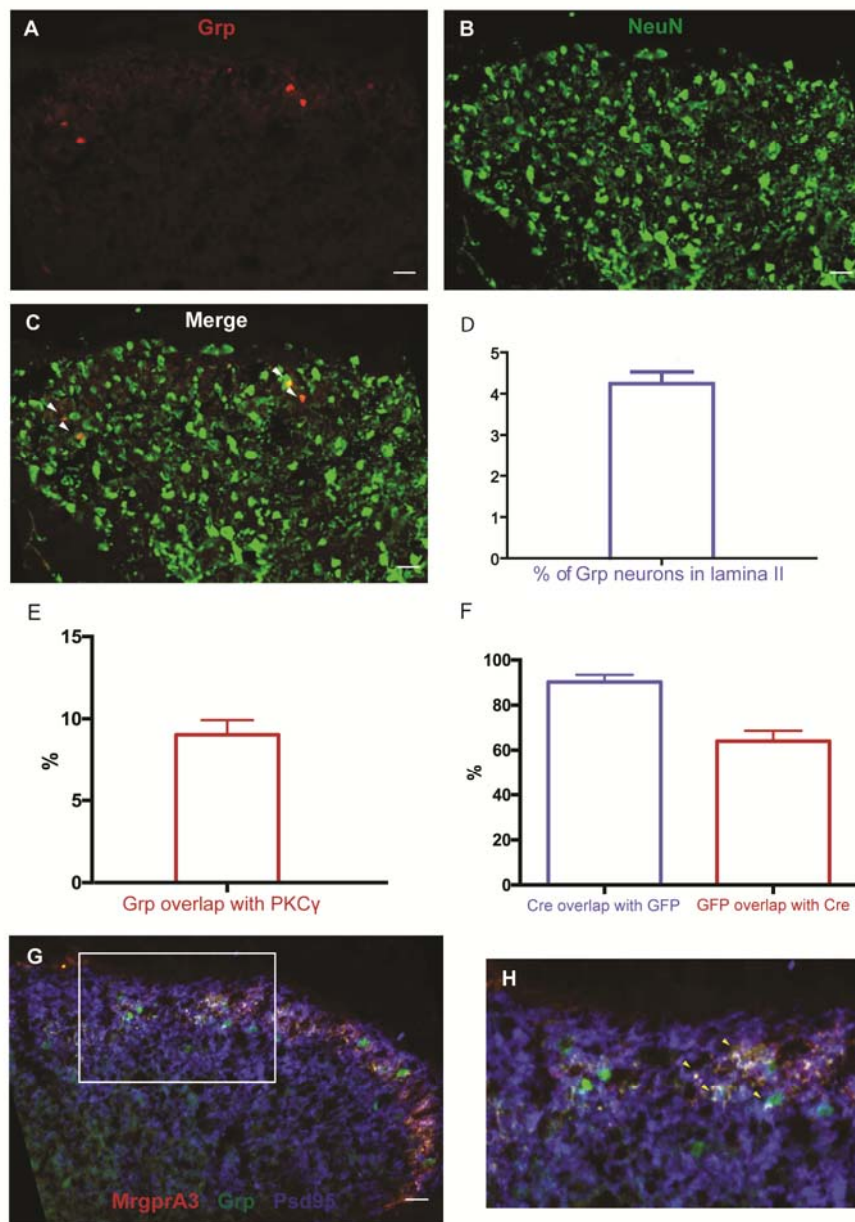


**Figure S1 Further characterization of *Grp*<sup>+</sup> neurons. Related to Figure 1.**

(A) Spinal cord sections from *Grp*<sup>Cre</sup>; *ROSA26*<sup>LSL-tdTomato</sup> mice, tdTomato fluorescence were visualized directly without staining. (B) NeuN staining. (C) Co-localization of *Grp*<sup>+</sup> neurons and NeuN staining. Arrowheads indicate overlap. (D) *Grp*<sup>+</sup> neurons represent 4.24% lamina II neurons (n = 25 hemisections from five mice). (E) Percentage of *Grp*<sup>+</sup> neurons positive for PKCγ (n=15 hemisections from three mice). (F) Percentage of *Grp*<sup>Cre</sup> positive neurons overlap with *Grp*<sup>EGFP</sup> positive neurons and percentage of *Grp*<sup>EGFP</sup> positive neurons overlap with *Grp*<sup>Cre</sup> positive neurons (n=15 hemisections from three mice). (G) Co-localization of *Grp*<sup>+</sup> neurons (green) with *MrgprA3* (red) and PSD95 (purple). (H) Representative neurons in boxed region in G shown at greater magnification. Arrowheads indicate co-localization of

*Grp*<sup>+</sup> neurons with *MrgprA3* central terminals and synaptic marker PSD95. Data are represented as mean ± SEM. All scale bars represent 20 μm.

Figure S2

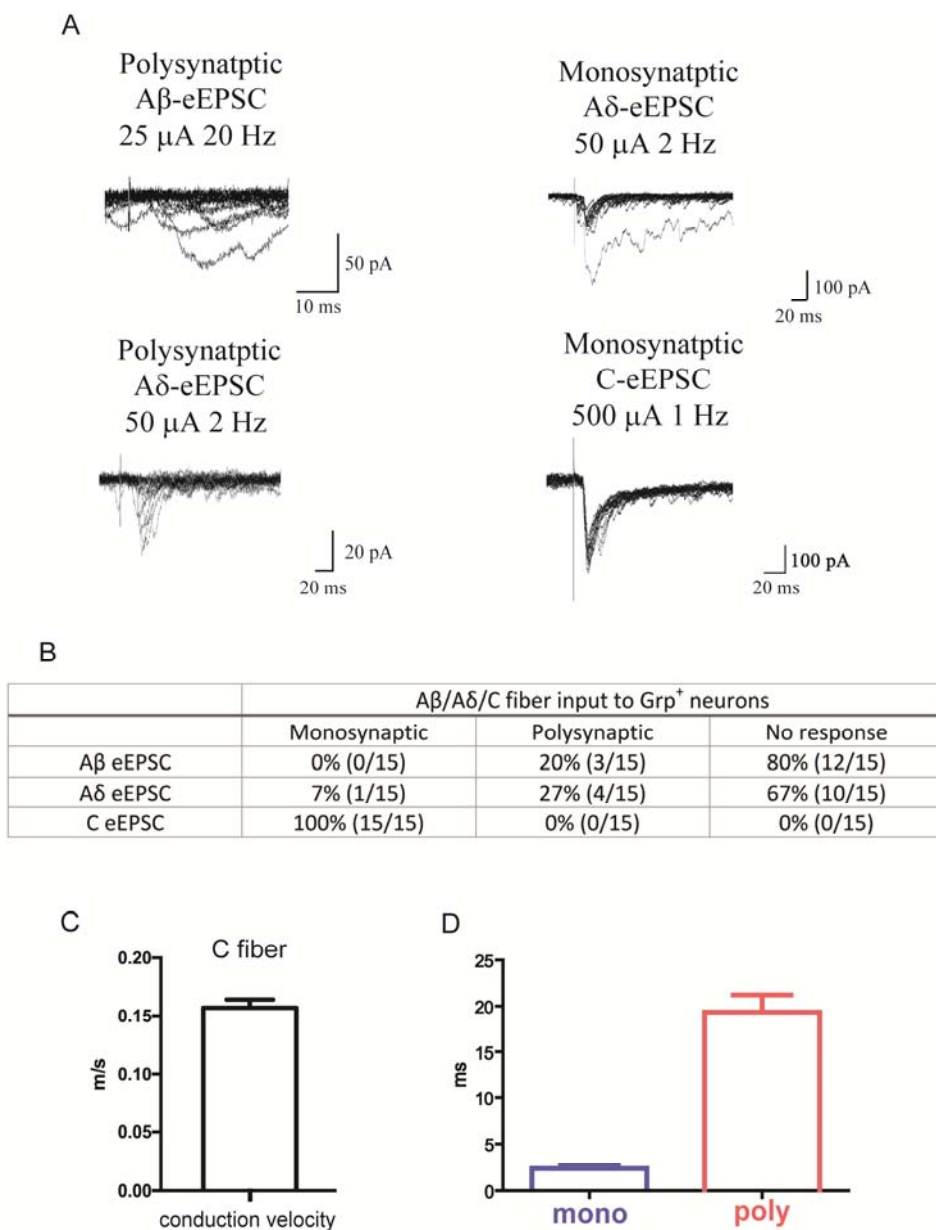
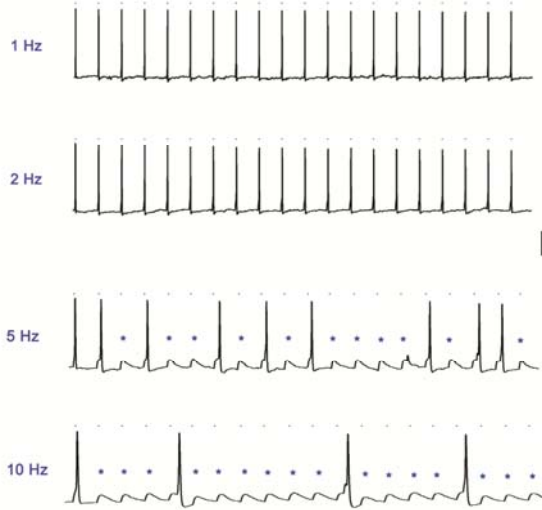


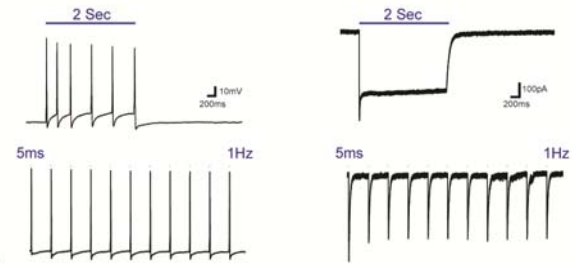
**Figure S2 Synaptic input to *Grp*<sup>+</sup> neurons. Related to Figure 2.**

(A) Representative traces of Aβ (25μA, 20Hz), Aδ (50μA, 2Hz) and C fiber (500μA, 1Hz) stimulation induced EPSC in *Grp*<sup>+</sup> neurons. (B) Summary of Aβ, Aδ and C fiber induced responses in *Grp*<sup>+</sup> neurons, categorized as monosynaptic, polysynaptic and no response. (C) Conduction velocities of C fiber input onto *Grp*<sup>+</sup> neurons (n=15). (D) Light activation of *MrgprA3*<sup>+</sup> neurons induced EPSC jitters in *Grp*<sup>+</sup> neurons (monosynaptic) and in *Grp* negative neurons (polysynaptic) (n=16 vs. 5).

Figure S3 A



B



C

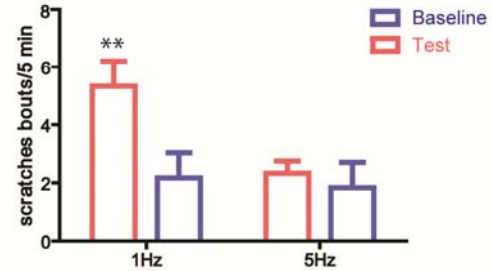


**Figure S3 Light-mediated *MrgprA3* activation. Related to Figure 2.**

(A) Light-evoked action potentials in cultured *MrgprA3*<sup>Cre</sup>; *ROSA26*<sup>LSL-ChR2</sup> DRG neurons. \* indicates failure of action potential. (B) Continuous and 1 Hz light induced responses in current clamp and voltage clamp mode. Blue bars indicate 5ms light stimulation. (C) Light-induced scratching bouts in *MrgprA3*<sup>Cre</sup>; *ROSA26*<sup>LSL-ChR2</sup> (test, n=6) compared with sham responses with no light (baseline, n=6). \*\*: P<0.01, two-tailed unpaired Student's t test. Data are represented as mean ± SEM.

Figure S4

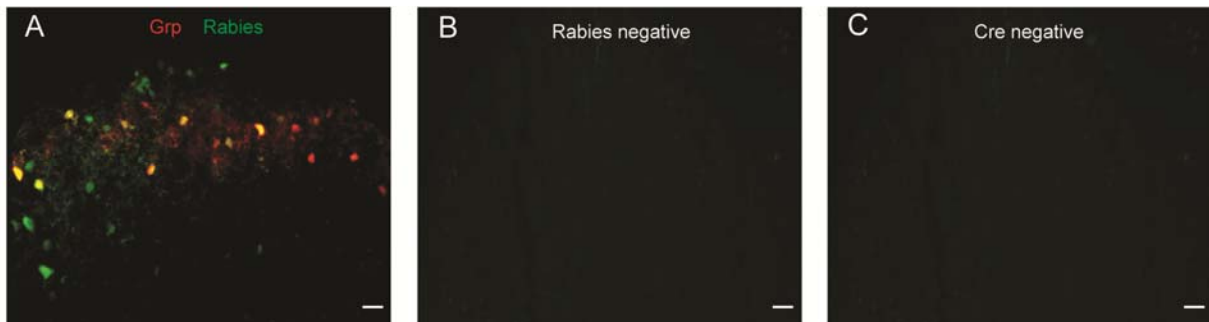


**Figure S4 Single synapse retrograde tracing from *Grp*<sup>+</sup> neurons. Related to Figure 3.**

(A) Rabies virus (green) infected *Grp*<sup>+</sup> neurons labeled by tdTomato fluorescence and surrounding neurons representing presynaptic targets of *Grp*<sup>+</sup> neurons. (B and C) Rabies virus cannot infect spinal cord neurons without helper virus or in Cre negative control mice. All scale bars represent 20 μm.

Figure S5

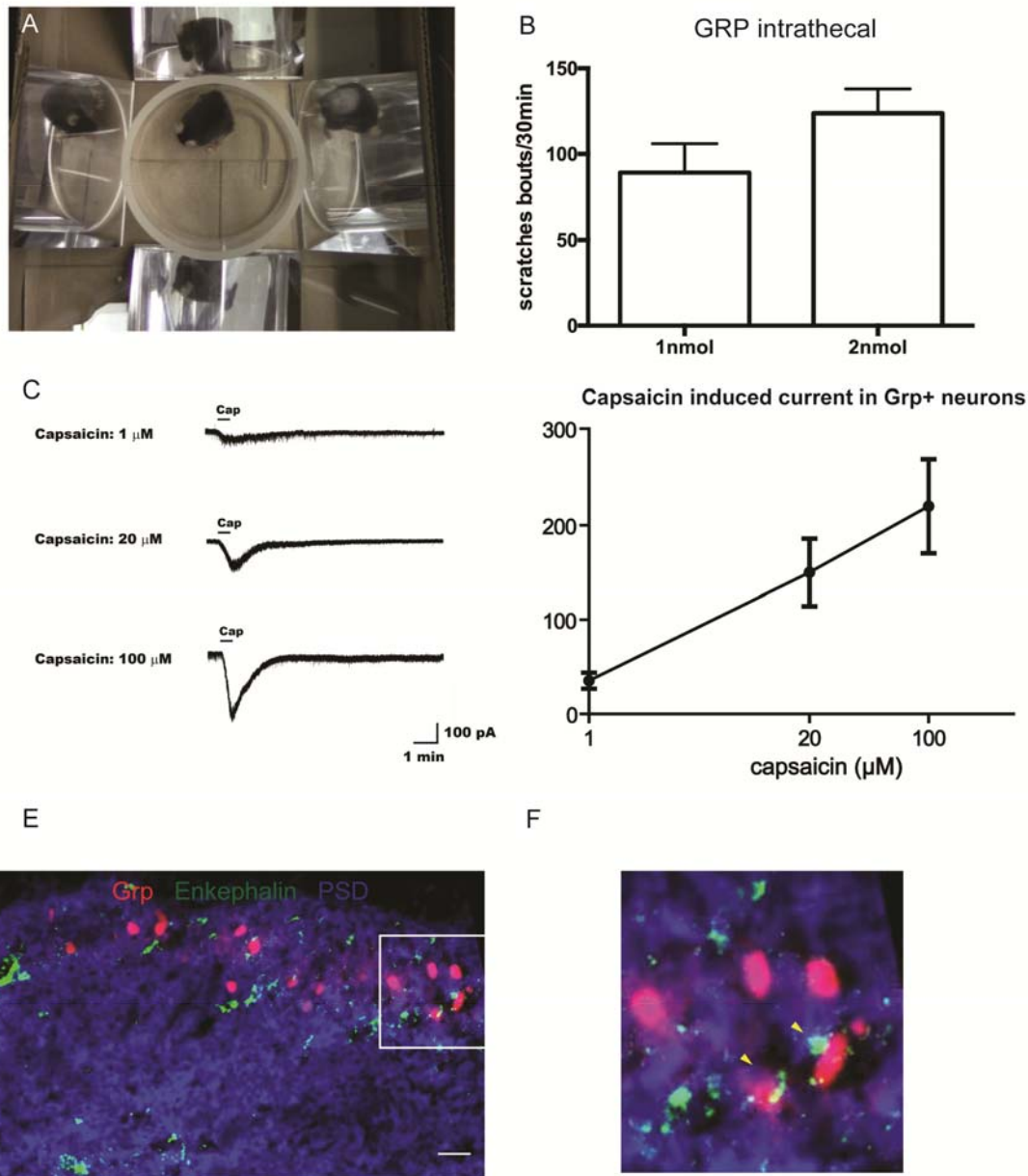


**Figure S5 Capsaicin-mediated activation of *Grp*<sup>+</sup> neurons and co-localization of *Grp*<sup>+</sup> neurons and enkephalin-expressing neurons. Related to Figure 5.**

(A) Photo showing behavior chamber with four mirrors on opposing sides with high-definition camera recording video from above. (B) 1nmol (n=4) and 2nmol (n=8) GRP intrathecal injection induced scratching response in wildtype mice. (C) Representative traces of capsaicin-induced EPSCs in *Grp*<sup>+</sup> neurons of *Grp*<sup>Cre</sup>; *ROSA26*<sup>LSL-TrpV1</sup>; *TrpV1*<sup>-/-</sup> spinal slices. Black bars indicate capsaicin application. (D) Capsaicin dose responses of *Grp*<sup>+</sup> neurons ectopically expressing TrpV1 (n=6 each dose). (E) Co-localization of *Grp*<sup>+</sup> neurons with enkephalin-expressing neurons and PSD95. (F) Representative neurons in boxed region in E shown at greater magnification. Arrowheads indicate *Grp*<sup>+</sup> neurons co-localized with Enkephalin and synaptic marker PSD95. Data are represented as mean ± SEM. All scale bars represent 20 μm.

Figure S6

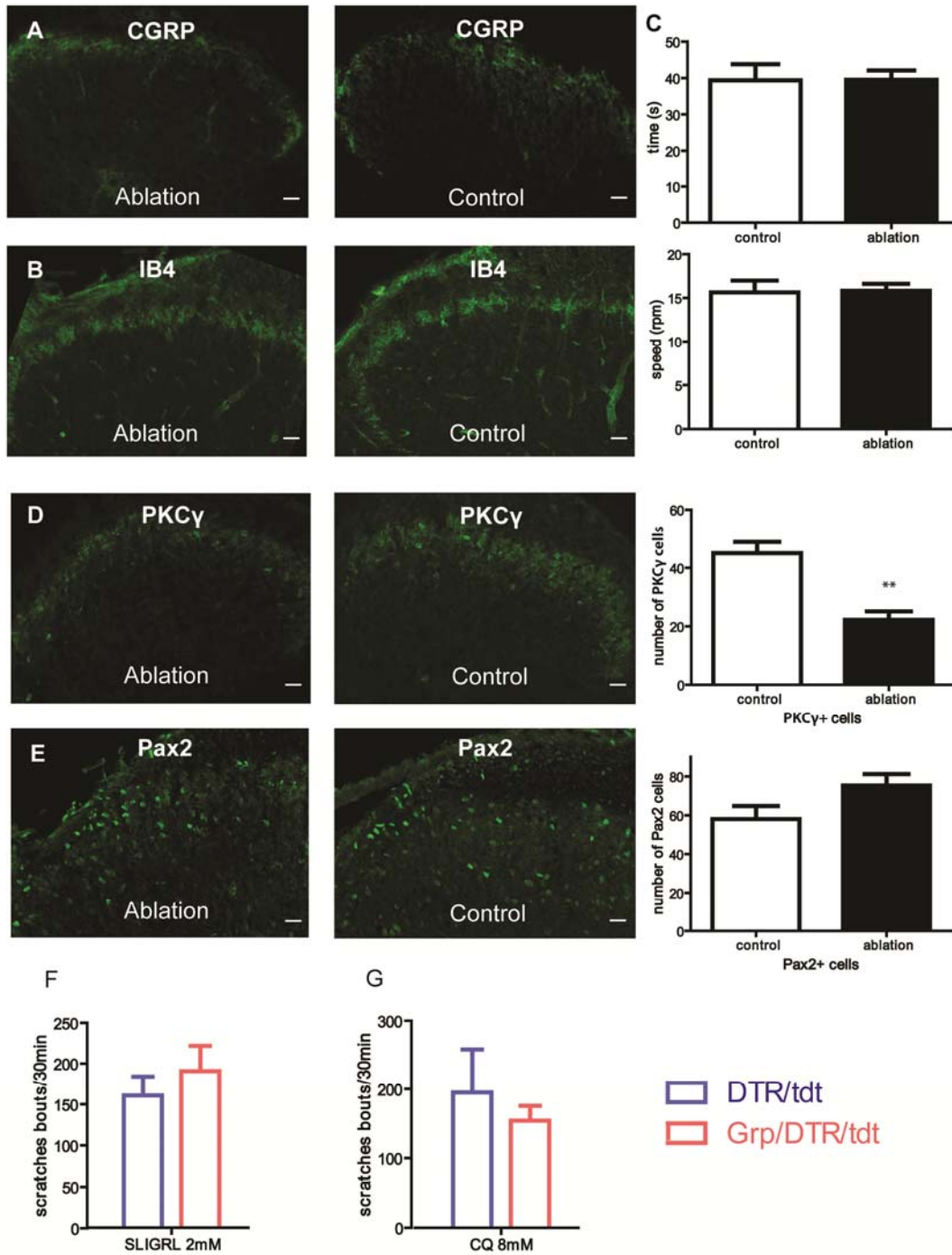


**Figure S6 Supplemental results for Grp ablation. Related to Figure 8.**

(A and B) Representative images of *Grp<sup>Cre</sup>; ROSA26<sup>LSL-DTR; LSL-tdTomato</sup>* (ablation) and *ROSA26<sup>LSL-DTR; LSL-tdTomato</sup>* (control) spinal cords stained with CGRP and IB4. (C) Ablation of *Grp<sup>+</sup>* neurons did not affect motor coordination in Rotarod tests (time and speed). (D and E) Representative images of PKC $\gamma$  and Pax2 positive neurons in *Grp<sup>Cre</sup>; ROSA26<sup>LSL-DTR; LSL-tdTomato</sup>* (ablation) and *ROSA26<sup>LSL-DTR; LSL-tdTomato</sup>* (control) spinal cords. Quantification on right panels. (F) Ablated mice showed reduced itch responses to low doses of SLIGRL (1mM) and CQ (4mM) (Fig 4D), while high doses (SLIGRL 2mM, n=8; CQ 8mM,

n=12 vs. 8) generated similar responses in both ablated and control mice. \*\*: P<0.01, two-tailed unpaired Student's t test. Data are represented as mean  $\pm$  SEM. All scale bars represent 20  $\mu$ m.

## Video legends

### **Video 1 Optogenetic activation of *MrgprA3*<sup>+</sup> neurons triggered scratching. Related to Figure 2.**

Baseline and blue light mediated activation of *MrgprA3*<sup>+</sup> neurons in *ROSA26*<sup>LSL-ChR2</sup> mice (control) and *MrgprA3*<sup>Cre</sup>; *ROSA26*<sup>LSL-ChR2</sup> mice (A3-ChR2) with shaved nape area.

### **Video 2 Activation of *Grp*<sup>+</sup> neurons generated pain and itch responses simultaneously. Related to Figure 5.**

Capsaicin-mediated specific activation of *Grp*<sup>+</sup> neurons in *Grp*<sup>Cre</sup>; *ROSA26*<sup>LSL-TrpVI</sup>; *TrpVI*<sup>-/-</sup> mice (1  $\mu$ g capsaicin intrathecally delivered). One fourth of the original speed. Pain-related licking (red) and itch-related scratching (blue) labeled in video.